Sudan University of Sciences and Technology

College of Graduate Studies

Measurement of Normal Thyroid Gland Volume in School Age Children using Ultrasonography

قياس حجم الغدة الدرقية الطبيعية لأطفال المدارس باستخدام التصوير بالموجات فوق الصوتية

A Thesis Submitted for Partial Fulfillment of the Requirements of M.Sc. Degree in Medical Diagnostic Ultrasound

By:

Samah Mohammed Bakry Mohammed

Supervisor:

Dr. Babiker Abd Elwahab Awad Alla Awad Elseed

2017

Dedication

To

My Family

My Husband

My Kids

Acknowledgment

First of all, I Thank Allah; the almighty for helping me to complete this project. I would like to thank Dr. Babiker Abd Elwahab Awad Alla, my supervisor for his helping and guidance, my great fullness for my all teachers in different educational levels.

Finally I would like to thank everybody who helped me in this project.

List of Contents

Chapter Three: Materials and Methods

Chapter Four: Results

Chapter Five: Discussion, Conclusion and Recommendations

List of Tables

List of Figures

List of Abbreviations

Abbreviation	Meaning
CT	Computed Tomography
ICCIDD	International Council for the Control of Iodine Deficiency Disorders
MRI	Magnetic Resonance Imaging
WHO	World Health Organization

ملخص البحث

هذه دراسة مستعرضه أجريت خلال الفترة من أغسطس إلى أكتوبر 2016 ، في مركز التشخيص الجراحي ، ولاية كسلا - السودان. ناقشت الدراسة قياس حجم الغدة الدرقية الطبيعي لأطفال المدارس باستخدام الموجات فوق الصوتية وربط هذا الحجم مع العمر والجنس والطول والوزن.

تم اختيار مجموعه "64" حاله عشوائيا تتراوح أعمارهم بين 6 إلى 18 سنة ,أي شخص يقل عمره عن 6 سنوات أو أكبر من 18 عامًا تم استبعاده كما تم استبعاد أي غدة درقية غير طبيعية من هذه الدراسة.

تم فحص جميع الحالات باستخدام جهاز الموجات فوق الصوتية ميندارى مع جهاز فحص 10. ميغاهرتز

.تم إجراء المسح بالموجات فوق الصوتية لجميع الحالات لتقييم أبعاد وحجم الغدة الدرقية ,كما تم جمع البيانات باستخدام ورقة جمع البيانات وتحليل البيانات باستخدام ، الانحدار الخطي والجدولة المتقاطعة والتحليل التمييزي.

أظهرت الدراسة أن متوسط القيم للطول و الوزن للجسم هو 138,07 ± 17,6، 33,83 ± 18,8 و 136 ± 16,9، 33,35 ± 16,05 للذكور والإناث على التوالي. وكان متوسط حجم .الغدة الدرقية لذكور والإناث 3,96 ± 1,28 سم 3

خلصت الدراسة إلى أن هناك دلالة إحصائية للفرق في قياسات الفصوص اليمنى واليسرى .بسبب العمر ومؤشر كتلة الجسم

كما كشفت الدراسة أيضا أن الفص الأيمن أكبر في الحجم من الأيسر ، وتبين قياسات الإناث .أن متوسط حجم الفصين أعلى من الذكور

أوصت الدراسة بما يلي: نصح جميع الأشخاص وخاصة الأطفال وأولئك الذين لديهم نقص في اليود لأجراء فحص دوري باستخدام الموجات فوق الصوتية لاستبعاد وجود أي خلل لأن الموجات فوق الصوتية آمنة ورخيصة الثمن و موثوق بها .

Abstract:

This is a retrospective cross sectional study which was done during the period from August to October 2016, at Surgical Diagnostic Center, Kassala state - Sudan. The study discussed measurement of normal thyroid volume in school age Sudanese using Ultrasonography and correlate this volume with age, gender, height and weight.

A total of "64" subjects were selected randomly; all those patients have age ranged from 6 to 18 years and with normal thyroid gland. Any subject had age fewer than 6 or above 18 years or had abnormal thyroid was excluded from this study.

All patients were subjected to be examined by U/S scanning using Mindray M7 color Ultrasound Machine with 10 MHz probe.

Ultrasound Scanning was performed for all subjects to evaluate thyroid dimensions and volume.

Data was collected using a data collecting sheet and in data analysis the author uses the cross tabulation, linear regression and discriminates analysis.

Study shows that the mean values for body characteristic height and weight were 138.07±17.6 ,33.83±18.8 and 136± 16.9 ,33.35±16.05 for male and female respectively. The overall mean thyroid gland volume combined for both lobes and sex obtained from this study was 3.96±1.28 cm^3.

Study concluded that; there was a statistical significance of difference in right and left lobes measurements due to age and body mass index.

Study also revealed that; the right lobe was larger in size than left one and female measurements show higher average size of two lobes than in males.

Study recommended that; All people specially child and those who have reduction of Iodine intake were advised to do U/S scanning routinely to exclude the presence of any abnormality, because U/S is a cheep, safety and reliable..

Chapter one

Introduction

1.1 Introduction:

Ultrasound has become one of the primary imaging modalities for the assessment of the major glands of internal secretion within the cervical region. The thyroid gland is among the most commonly imaged glands using ultrasound due to the limitation of clinical examination (Archie 1996).

Computed tomography (CT) and magnetic resonance imaging (MRI) provide structural information of the thyroid gland just like ultrasound but are relatively more expensive. Thyroid ultrasound appears suitable in tropical Africa where more sophisticated modern imaging techniques may not be readily available or are very expensive (Anele, 2001).

Anatomically, the normal thyroid gland consists of two lobes which lie on the anterolateral surface of the trachea extending from the thyroid cartilage superiorly to the sixth tracheal ring inferiorly. They are asymmetrical with the right lobe being larger than the left, and the thyroid gland is larger in males (Ryan, 1994).

In recent decades, sonography has become the gold standard for assessment of the thyroid gland (Massol, 1993).

Sonography has improved with the development of high-frequency transducers, which allow a more detailed study of the thyroid gland (Braneton, 1994).

As a result, the World Health Organization (WHO) and the International Council for the Control of Iodine Deficiency Disorders (ICCIDD) now consider sonography the diagnostic method for assessment of goiter. It is most often used in assessing the incidence of goiter in Third World populations, especially in children (WHO,ICCIDD, 1997).

Volumetric evaluation of the thyroid gland is based on the use of an ellipsoid model. Hence, a value is obtained that replaces clinical evaluation of volume. With the ellipsoid model, the height, the width, and the depth of

each lobe are measured and multiplied. The obtained result is then multiplied by a correction factor (Bron ,1978).

In Sudan, there is absence of domestic reference for thyroid volumes in school age ; in Sudan, as far as we know, no study was published in the open literature, regarding the thyroid volume in school age.

This study aimed to establish a local reference of thyroid volume in school age Sudanese normal subjects using ultrasound.

1.2 Problem:

There is no previous local study in normal thyroid gland dimensions and volume for Sudanese (school age).

1.3 Objectives:

1.3.1General objectives:

Measurement of normal thyroid gland volume in school age children using ultrasonography

1.3.2 Specific objectives:

- To correlate thyroid gland volume with gender, age ,height and weight
- To compare between thyroid volume in male and female for school age.
- To compare RT lobe size with LT lobe size of thyroid gland

1.4 Over view of the study:

This study include five chapters, chapter one, which was an introduction, deals with theoretical framework of the study. It present the statement of the study problems , objectives of this study , chapter two includes theoretical background and previous study , while chapter three discusses the material and method then chapter four include the results and finally chapter five consists of discussion , conclusion , recommendations, references and appendices.

Chapter Two

Background and Literature Review

Literature Review

2.1 Anatomy of the thyroid gland:

The thyroid is a highly vascular, brownish-red gland located anteriorly in the lower neck, extending from the level of the fifth cervical vertebra down to the first thoracic. The gland varies from an H to a U shape and is formed by 2 elongated lateral lobes with superior and inferior poles connected by a median isthmus, with an average height of 12-15 mm, overlying the second to fourth tracheal rings.

Each lobe is 50-60 mm long, with the superior poles diverging laterally at the level of the oblique lines on the laminae of the thyroid cartilage. The lower poles diverge laterally at the level of the fifth tracheal cartilage. Although thyroid weight varies, it averages 25-30 g in adults (cummings, 1998)

2.1.1 Development:

The thyroid gland is the first of the body's endocrine glands to develop, on approximately the 24th day of gestation. The thyroid originates from two main structures: the primitive pharynx and the neural crest. The rudimentary lateral thyroid develops from neural crest cells, while the median thyroid, which forms the bulk of the gland, arises from the primitive pharynx (Taknnashi, 2015).

The thyroid gland forms as a proliferation of endodermal epithelial cells on the median surface of the developing pharyngeal floor. The site of this development lies between 2 key structures, the tuberculum impar and the copula, and is known as the foramen cecum. The thyroid initially arises caudal to the tuberculum impar, which is also known as the median tongue bud. This embryonic swelling develops from the first pharyngeal arch and occurs midline on the floor of the developing pharynx, eventually helping form the tongue as the two lateral lingual swellings overgrow it.

The foramen cecum begins rostral to the copula, also known as the hypobranchial eminence. This median embryologic swelling consists of mesoderm that arises from the second pharyngeal pouch (although the third and fourth pouches are also involved). The thyroid gland, therefore, originates from between the first and second pouches.

The initial thyroid precursor, the thyroid primordium, starts as a simple midline thickening and develops to form the thyroid diverticulum. This structure is initially hollow, although it later solidifies and becomes bilobed. The stem usually has a lumen, the thyroglossal duct, that does not descend into the lateral lobes. The 2 lobes are located on either side of the midline and are connected via an isthmus (Gager, 2001).

2.1.2 Relations:

The thyroid gland lies in front of the neck, hidden by the anterior muscles of the neck, sternothyroid andsternohyoid muscles. It usually weighs 25g but this varies, as the gland is slightly heavier in females, and enlarges during menstruation and pregnancy. Estimation of the size of the thyroid gland by diagnostic ultrasound is important clinically, so as to evaluate and manage thyroid disorders. The anterior border of the gland is thin, the posterior border is rounded and related inferiorly to the inferior thyroid artery (cummings, 1998).

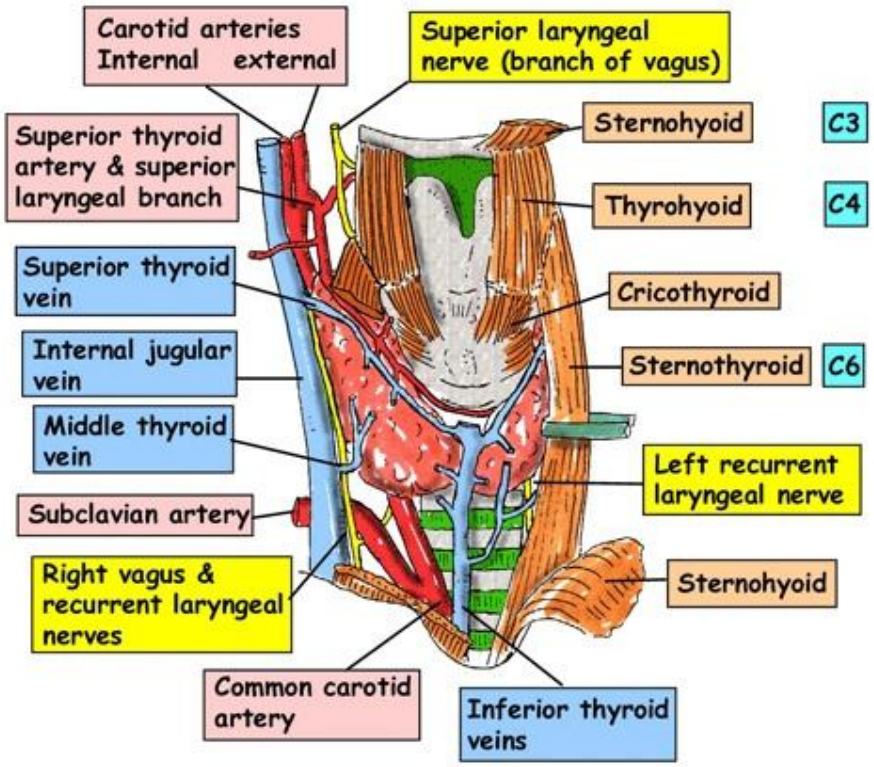

Figure 2.1 Anterior view of the thyroid gland with the infra hyoid muscles reflected (cummings, 1998).

The lateral surface is covered by the sternothyroid muscle, which is attached to the oblique line of the thyroid cartilage preventing the upper pole of the gland from extending onto the thyrohyoid muscle.

Anteriorly: Pretracheal fascia, sternohyoid muscle and the superior belly of omohyoid muscle. Overlapped inferiorly by the anterior border of the sterno-cleidomastoid muscle.

Medially: Recurrent laryngeal nerve, trachea, larynx and oesophagus. The superior pole of the gland contacts the inferior pharyngeal constrictor and superior part of cricothyroid. The external laryngeal nerve runs medial to the superior pole to supply the cricothyroid muscle.

Posteriorly: Prevertebral fascia, carotid sheath, parathyroid glands and trachea.

The isthmus is covered by sternothyroid and is separated from it by pretreachial fascia. The superior thyroid arteries anastomose along its upper border and the inferior thyroid veins leave the thyroid gland at its lower border (cummings, 1998).

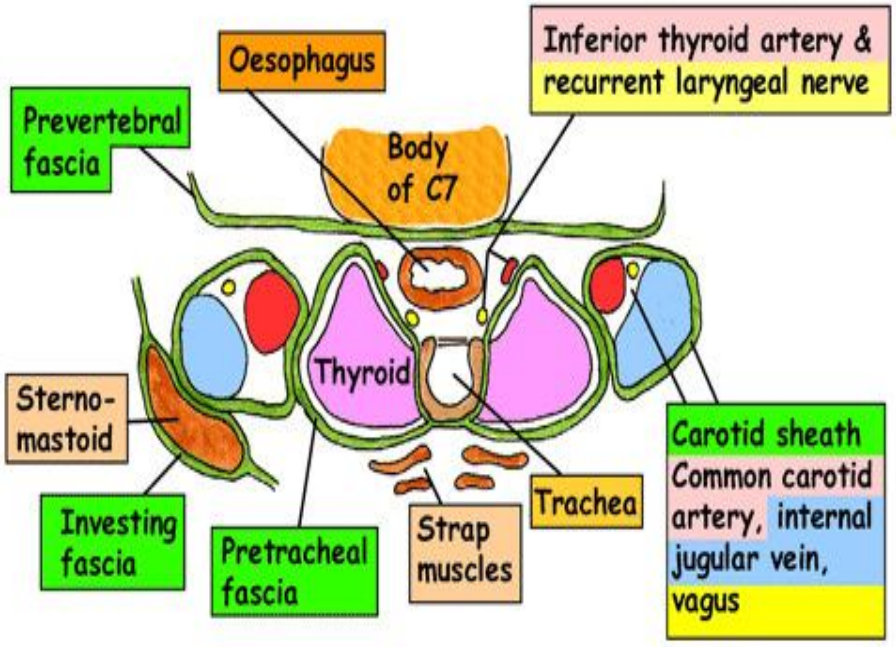

Figure2.2 Transverse section at C7 vertebrae level (cummings, 1998).

2.1.3 Structure:

Under the middle layer of deep cervical fascia, the thyroid has an inner true capsule, which is thin and adheres closely to the gland. Extensions of this capsule within the substance of the gland form numerous septae, which divide it into lobes and lobules. The lobules are composed of follicles, the structural units of the gland, which consist of a layer of simple epithelium enclosing a colloid-filled cavity.

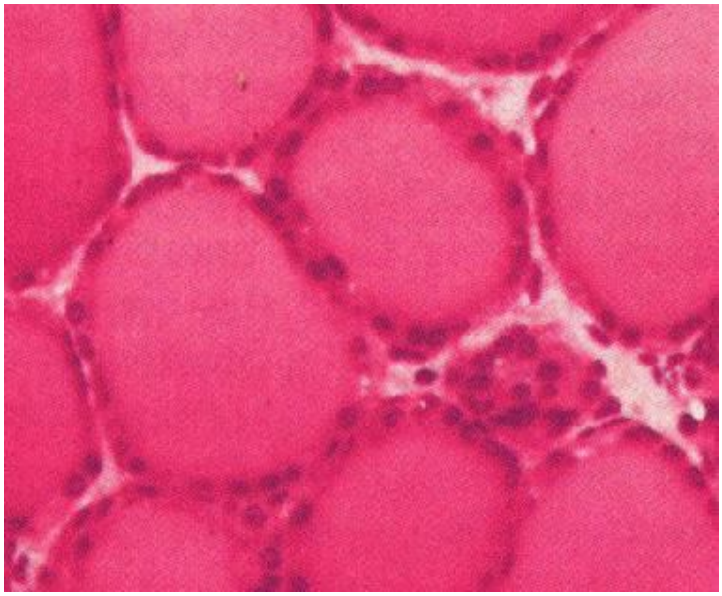

Figure2.3 Follicles of the thyroid gland, consisting of a layer of simple epithelium enclosing a colloid-filled cavity(Willims, 1995).

This colloid (pink on hematoxylin and eosin [H&E] stain) contains an iodinated glycoprotein, iodothyroglobulin, a precursor of thyroid hormones. Follicles vary in size, depending upon the degree of distention, and they are surrounded by dense plexuses of fenestrated capillaries, lymphatic vessels, and sympathetic nerves.

Epithelial cells are of 2 types: principal cells (ie, follicular) and parafollicular cells (ie, C, clear, light cells). Principal cells are responsible for formation of the colloid (iodothyroglobulin), whereas parafollicular cells produce the hormone calcitonin, a protein central to calcium homeostasis. Parafollicular cells lie adjacent to the follicles within the basal lamina (Willims, 1995).

2.1.4 Blood vessels of the thyroid gland:

The thyroid gland secretes hormones directly into the blood. Therefore it needs to be highly vascularised. Blood supply to the thyroid gland is achieved by two main arteries; the superior and inferior thyroid arteries. These are paired arteries arising on both the left and right.

The superior thyroid artery is the first branch of the external carotid artery. After arising, the artery descends toward the thyroid gland. As a generalisation, it supplies the superior and anterior portions of the gland.

The inferior thyroid artery arises from the thyrocervical trunk (which in turn is a branch of the subclavian artery). The artery travels superomedially to reach the inferior pole of the thyroid. It tends to supply the postero-inferior aspect.

In a small proportion of people (around 10%), there is an additional artery present; the thyroid ima artery. It comes from the brachiocephalic trunk of the arch of aorta, supplying the anterior surface and isthmus.

Venous drainage is carried out by the superior, middle and inferior thyroid veins, which form a venous plexus. The superior and middle veins drain into the internal jugular veins, whereas the inferior drains intothe brachiocephalic vein (Reed, 1943).

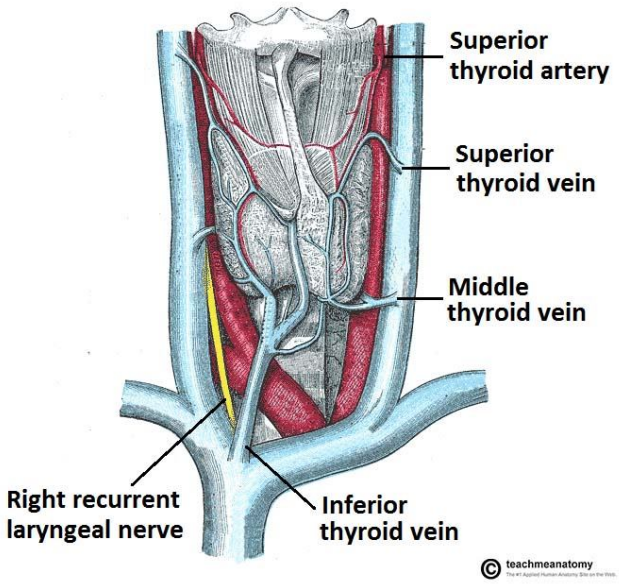

Figure 2.4Vasculature of the thyroid gland. The inferior thyroid artery is not visible from this anterior view(Reed

2.2 Functions of the thyroid gland:

2.2.1 Thyroid hormones

The primary function of the thyroid is the production of the iodine-containing thyroid hormones, triiodothyronine (T3) and thyroxine (T4) and the peptide hormone calcitonin (Dvidson, 2010) . T3 is so named because it contains three atoms of iodine per molecule and T4 contains four atoms of iodine per molecule(Gyton, Hall 2011) The thyroid hormones have a wide range of effects on the human body. These include:

2.2.1.1 Metabolic:

The thyroid hormones increase the basal metabolic rate and have effects on almost all body tissues.Appetite, the absorption of substances, and gut motility are all influenced by thyroid hormones. They increase the absorption in the gut, generation, uptake by cells, and breakdown of glucose. They stimulate the breakdown of fats, and increase the number of free fatty acids. Despite increasing free fatty acids, thyroid hormones decrease cholesterol levels, perhaps by increasing the rate of secretion of cholesterol in bile. (Gyton and Hall, 2011)

2.2.1.2 Cardiovascular:

The hormones increase the rate and strength of the heartbeat. They increase the rate of breathing, intake and consumption of oxygen, and increase the activity of mitochondria. Combined, these factors increase blood flow and the body's temperature.

2.2.1.3 Developmental:

Thyroid hormones are important for normal development.They increase the growth rate of young people,and cells of the developing brain are a major target for the thyroid hormones T3 and T4. Thyroid hormones play a particularly crucial role in brain maturation during fetal development.

The thyroid hormones also play a role in maintaining normal sexual function, sleep, and thought patterns. Increased levels are associated with

increased speed of thought generation but decreased focus.Sexual function, including libido and the maintenance of a normal menstrual cycle, are influenced by thyroid hormones.

After secretion, only a very small proportion of the thyroid hormones travel freely in the blood. Most are bound to thyroxine-binding globulin (about 70%), transthyretin (10%), and albumin (15%). Only the 0.03% of T4 and 0.3% of T3 traveling freely has hormonal activity. In addition, up to 85% of the T3 in blood is produced following conversion from T4 by iodothyronine deiodinases in organs around the body.(Davidson, 2010)

Thyroid hormones act by crossing the cell membrane and binding to intracellular nuclear thyroid hormone receptors TR-α1,TR-α2,TR-β1 and TR-β2, which bind with hormone response elements and transcription factors to modulate DNA transcription. In addition to these actions on DNA, the thyroid hormones also act within the cell membrane or within cytoplasm via reactions with enzymes,including calcium ATPase, adenylyl cyclase, and glucose transporters.(Greenspan, 2011)

2.2.2 Hormone production:

Synthesis of the thyroid hormones, as seen on an individual thyroid follicular cell, Thyroglobulin is synthesized in the rough endoplasmic reticulum and follows the secretory pathway to enter the colloid in the lumen of the thyroid follicle by exocytosis. Meanwhile, a sodium-iodide (Na/I) symporter pumps iodide (I^-) actively into the cell, which previously has crossed the endothelium by largely unknown mechanisms. This iodide enters the follicular lumen from the cytoplasm by the transporter pendrin, in a purportedly passive manner. In the colloid, iodide (I^-) is oxidized to iodine (I0) by an enzyme called thyroid peroxidase. Iodine (I0) is very reactive and iodinates the thyroglobulin at tyrosyl residues in its protein chain (in total containing approximately 120 tyrosyl residues). In conjugation, adjacent tyrosyl residues are paired together. The entire complex re-enters the

follicular cell by endocytosis and Proteolysis by various proteases liberates thyroxine and triiodothyronine molecules, which enters the blood by largely unknown mechanisms.

The thyroid hormones are created from thyroglobulin. This is a protein within the follicular space that is originally created within the rough endoplasmic reticulum of follicular cells and then transported into the follicular space. Thyroglobulin contains 123 units of tyrosine, which reacts with iodine within the follicular space.

Iodine is essential for the production of the thyroid hormones. Iodine (I0) travels in the blood as iodide (I^-), which is taken up into the follicular cells by a sodium-iodide symporter. This is an ion channel on the cell membrane which in the same action transports two sodium ions and an iodide ion into the cell. Iodide then travels from within the cell into the follicular space, through the action of pendrin, an iodide chlo-ride antiporter. In the follicular space, the iodide is then oxidized to iodine. This makes it more reactive, and the iodine is attached to the active tyrosine units in thyroglobulin by the enzyme thyroid peroxidase. This forms the precursors of thyroid hormones monoiodotyrosine (MIT), and diiodotyrosine (DIT).

When the follicular cells are stimulated by thyroid-stimulating hormone, the follicular cells reabsorb thyroglobulin from the follicular space. The iodinated tyrosines are cleaved, forming the thyroid hormones T4, T3, DIT, MIT, and traces of reverse triiodothyronine. T3 and T4 are released into the blood. The hormones secreted from the gland are about 80–90% T4 and about 10–20% T3. Deiodinase enzymes in peripheral tissues remove the iodine from MIT and DIT and convert T4 to T3 and RT3. This is a major source of both RT3 (95%) and T3 (87%) in peripheral tissues.(Bron 2003).

2.2.3 Regulation:

The production of thyroxine and triiodothyronine is primarily regulated by thyroid-stimulating hormone (TSH), released by the anterior pituitary gland. TSH release in turn is stimulated by thyrotropin releasing hormone (TRH), released in a pulsatile manner from the hypothalamus.

The thyroid hormones provide negative feedback to the thyrotropes TSH and TRH: when the thyroid hormones are high, TSH production is suppressed. This negative feedback also occurs when levels of TSH are high, causing TRH production to be suppressed.

TRH is secreted at an increased rate in situations such as cold exposure in order to stimulate thermogenesis.In addition to being suppressed by the presence of thyroid hormones, TSH production is blunted by dopamine, somatostatin, and glucocorticoids (Bron, 2003).

2.2.4Calcitonin:

The thyroid gland also produces the hormone calcitonin, which helps regulate blood calcium levels. Parafollicular cells produce calcitonin in response to high blood calcium. Calcitonin decreases the release of calcium from bone, by decreasing the activity of osteoclasts, cells which break bone down. Bone is constantly reabsorbed by osteoclasts and created by osteoblasts, so calcitonin effectively stimulates movement of calcium into bone. The effects of calcitonin are opposite those of the parathyroid hormone, produced in the parathyroid glands. However, calcitonin seems far less essential than PTH, as calcium metabolism remains clinically normal after removal of the thyroid (thyroidectomy), but not the parathyroid glands (Bron, 2003).

2.3 Investigations done for thyroid gland:

2.3.1 laboratory Investigations:

2.3.1.1 Thyroid Stimulating Hormone:

Single best test for thyroid disease. When T3 & T4 are high TSH is low. When t3 & T4 are low, TSH is high Use of TSH level , Diagnosis & follow , up of thyroid dysfunction

2.3.1.2 Thyroid function test TFT:

Is a collective term for blood test used to check the function of the thyroid

TFTs may be requested if a patient is thought to suffer from hyper thyroidism (overactive thyroid) or hypothyroidism (underactive thyroid), or to monitor the effectiveness of either thyroid-suppression or hormone replacement therapy. It is also requested routinely in conditions linked to thyroid disease, such as atrial fibrillation and anxiety disorder.

A TFT panel typically includes thyroid hormones such as thyroid stimulating hormone (TSH, thyrotropin) and thyroxine (T4), and triiodo-thyronine (T3) (Dayan, 2001).

2.3.1.3 Serum Antibodies Inhibiting antibodies:

Anti thyroglobulin -Anti peroxidase to exclude Hashimotos Thyroiditis (Dayan, 2001).

2.3.2 Radiological Investigations:

2.3.2.1 Radionuclide scan:

The radioactive iodine uptake test, or RAIU test, is a type of scan used in the diagnosis of thyroid problems, particularly hyperthyroidism.. The RAIU test is also used as a follow up to RAI therapy to verify that no thyroid cells survived, which could still be cancerous.

The patient swallows a radioisotope of iodine in the form of capsule or fluid, and the absorption (uptake) of this radiotracer by the thyroid is studied after

4–6 hours and after 24 hours with the aid of a scintillation counter. The dose is typically 0.15–0.37 MBq (4–10 μCi) of 131I sodium iodide, or 3.7–7.4 MBq (100–200 μCi) of 123I sodium iodide.

The normal uptake is between 15 and 25 percent, but this may be forced down if, in the meantime, the patient has eaten foods high in iodine, such as dairy products and seafood.] Low uptake suggests thyroiditis, high uptake suggests Graves' disease, and unevenness in uptake suggests the presence of a nodule (Kwee, 2007).

2.3.2.2 CT & MRI:

Rarely indicated, only to evaluate retro sternal extension.

2.3.2.3 PET:

Using fluorodeoxy glucose F18,it can diffrenitate benign from malignant but highly expensive and cannot replace biopsy(Sallie, 2006).

2.3.2.4 Thyroid Ultrasound:

High-frequency transducers (7.5-15.0 MHz) currently provide both deep ultrasound penetration—up to 5 cm—and high-definition images, with a resolution of 0.5 to 1.0 mm. No other imaging method can achieve this degree of spatial resolution. Linear array transducers with either rectangular or trapezoidal scan format are preferred to sector transducers because of the wider near field of view and the capability to combine high frequency gray-scale and color Doppler images. The thyroid gland is one of the most vascular organs of the body. As a result, Doppler examination may provide useful diagnostic information in some thyroid diseases.

2.4 Basic ultrasound physics:

All diagnostic ultrasound applications are based on the detection and display of acoustic energy reflected from interfaces within the body. These interactions provide the information needed to generate high-resolution, gray-scale images of the body, as well as display information related to blood flow.

2.4.1 Wavelength and Frequency:

Sound is the result of mechanical energy traveling through matter as a wave producing alternating compression and rarefaction. Pressure waves are propagated by limited physical displacement of the material through which the sound is being transmitted. A plot of these changes in pressure is a sinusoidal waveform, in which the Y axis indicates the pressure at a given point and the X axis indicates time. Changes in pressure with time defied the basic units of measurement for sound. The distance between corresponding points on the time pressure curve is defined as the wavelength (λ), and the time (T) to complete a single cycle is called the period. The number of complete cycles in a unit of time is the frequency *(f)* of the sound. Frequency and period are inversely related. If the period (T) is expressed in seconds, $f = 1/T$, or $f = T \times sec{-}1$. The unit of acoustic frequency is the hertz (Hz); 1 Hz = 1 cycle per second. High frequencies are expressed in kilohertz (kHz; 1 kHz = 1000 Hz) or megahertz (MHz; 1 MHz = 1,000,000 Hz). In nature, acoustic frequencies span a range from less than 1 Hz to more than 100,000 Hz (100 kHz). Human hearing is limited to the lower part of this range, extending from 20 to 20,000 Hz. Ultrasound differs from audible sound only in its frequency, and it is 500 to 1000 times higher than the sound we normally hear. Sound frequencies used for diagnostic applications typically range from 2 to 15 MHz, although frequencies as high as 50 to 60 MHz are under investigation for certain specialized imaging applications. In general, the frequencies used for ultrasound imaging are higher than those used for Doppler.

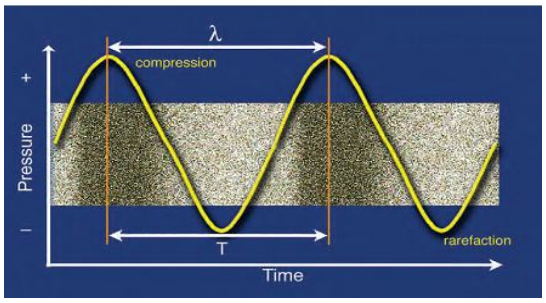

Figure 2.5 Shows sound wave

2.4.2 Propagation of Sound:

In most clinical applications of ultrasound, brief bursts or pulses of energy are transmitted into the body and propagated through tissue. Acoustic pressure waves can travel in a direction perpendicular to the direction of the particles being displaced (transverse waves), but in tissue and fluids, sound propagation is along the direction of particle movement (longitudinal waves). The speed at which the pressure wave moves through tissue varies greatly and is affected by the physical properties of the tissue. Propagation velocity is largely determined by the resistance of the medium to compression, which in turn is influenced by the density of the medium and its stiffness or elasticity. Propagation velocity is increased by increasing stiffness and reduced by decreasing density. In the body, propagation velocity may be regarded as constant for a given tissue and is not affected by the frequency or wavelength of the sound.

2.4.3 Distance Measurement:

Propagation velocity is a particularly important value in clinical ultrasound and is critical in determining the distance of a reflecting interface from the transducer. Much of the information used to generate an ultrasound scan is based on the precise measurement of time and employs the principles of **echo-ranging.** If an ultrasound pulse is transmitted into the body and the time until an echo returns is measured, it is simple to calculate the depth of the interface

that generated the echo, provided the propagation velocity of sound for the tissue is known.

2.4.4 Acoustic impedance (Z):

Is determined by product of the density (ρ) of the medium propagating the sound and the propagation velocity (c) of sound in that medium ($Z = \rho c$). Interfaces with large acoustic impedance differences, such as interfaces of tissue with air or bone, reflect almost all the incident energy. Interfaces composed of substances with smaller differences in acoustic impedance, such as a muscle and fat interface, reflect only part of the incident energy.

2.4.5 Reflection:

The way ultrasound is reflected when it strikes an acoustic interface is determined by the size and surface features of the interface. If large and relatively smooth, the interface reflects sound much as a mirror reflects light. Such interfaces are called **specular reflectors** because they behave as "mirrors for sound." The amount of energy reflected by an acoustic interface can be expressed as a fraction of the incident energy; this is termed the **reflection coefficient** (R). If a specular reflector is perpendicular to the incident sound beam, the amount of energy reflected is determined by the following relationship: $R = (Z2-Z1)2 / (Z2 + Z1)2$

where Z1 and Z2 are the acoustic impedances of the media forming the interface.

Because ultrasound scanners only detect reflections that return to the transducer, display of specular interfaces is highly dependent on the angle of insonation (exposure to ultrasound waves). Specular reflectors will return echoes to the transducer only if the sound beam is perpendicular to the interface. If the interface is not at a 90-degree angle to the sound beam, it will be reflected away from the transducer, and the echo will not be detected. Most

echoes in the body do not arise from specular reflectors but rather from much smaller interfaces within solid organs. In this case the acoustic interfaces involve structures with individual dimensions much smaller than the wavelength of the incident sound. The echoes from these interfaces are scattered in all directions. Such reflectors are called diffuse reflectors and account for the echoes that form the characteristic echo patterns seen in solid organs and tissues. The constructive and destructive interference of sound scattered by diffuse reflectors results in the production of ultrasound speckle, a feature of tissue texture of sonograms of solid organs. For some diagnostic applications, the nature of the reflecting structures creates important conflicts. For example, most vessel walls behave as specular reflectors that require insonation at a 90-degree angle for best imaging, whereas Doppler imaging requires an angle of less than 90 degrees between the sound beam and the vessel.

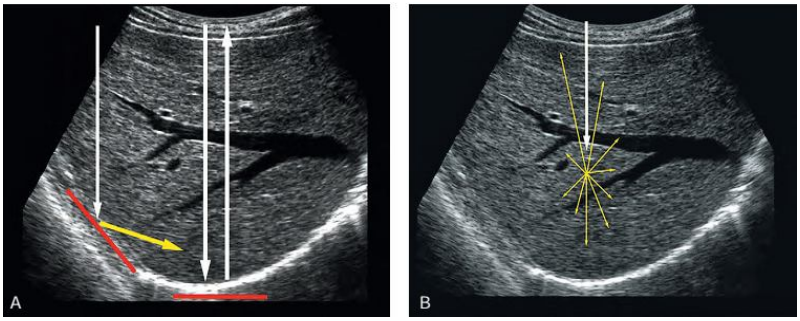

Figure 2.6 Ultrasound images represent A, Specular reflector. B, Diffuse reflector

2.4.6 Refraction:

Another event that can occur when sound passes from a tissue with one acoustic propagation velocity to a tissue with a higher or lower sound velocity

is a change in the direction of the sound wave. This change in direction of propagation is called refraction and is governed by Snell's law:

$Sin^{0}1 / Sin\ ^{0}2 = C1/C2$

Where **$^{0}1$** is the angle of incidence of the sound approaching the interface, **$^{0}2$** is the angle of refraction, and c1 and c2 are the propagation velocities of sound in the media forming the interface.

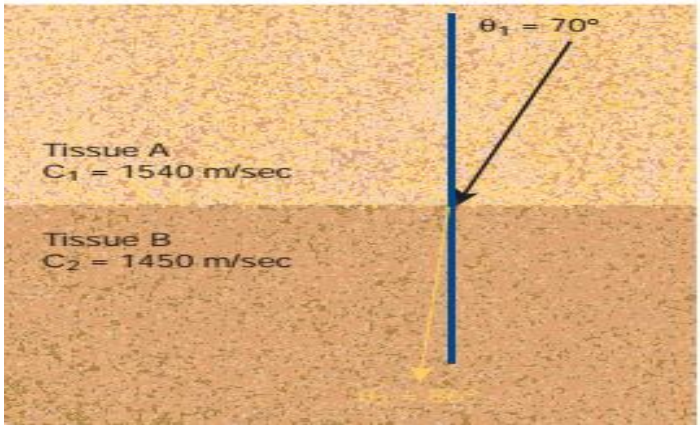

Figure 2.7 Shows Refraction.

2.4.7 Attenuation:

An ultrasound wave can be attenuated by several mechanisms as it travels through tissue. The most important mechanism is absorption, in which ultrasound energy is converted into heat. In most diagnostic systems, ultrasound propagates in the form of a beam. The attenuation of practical interest is the rate at which ultrasound intensity in the beam decreases with distance. As well as absorption, the intensity in the beam may be reduced due to scattering of ultrasound out of the beam and to divergence or spreading of the beam with distance. Attenuation depends on the insonating frequency as well as the nature of the attenuating medium. High frequencies are attenuated more rapidly than lower frequencies, and transducer frequency is a major determinant of the useful depth from which information can be obtained with

ultrasound. Attenuation determines the efficiency with which ultrasound penetrates a specific tissue and varies considerably in normal tissues.

Intensity (I) is used to describe the spatial distribution of power and is calculated by dividing the power by the area over which the power is distributed, as follows: **I (W/ cm2) = Power (W) / Area (cm2)**

The **attenuation** of sound energy as it passes through tissue is of great clinical importance because it influences the depth in tissue, from which useful information can be obtained. This in turn affects transducer selection and

a number of operator-controlled instrument settings, including time (or depth) gain compensation, power output attenuation, and system gain levels. Attenuation is measured in relative rather than absolute units. The **decibel** (dB) notation is generally used to compare different levels of ultrasound power or intensity. This value is 10 times the log10 of the ratio of the power or intensity values being compared.

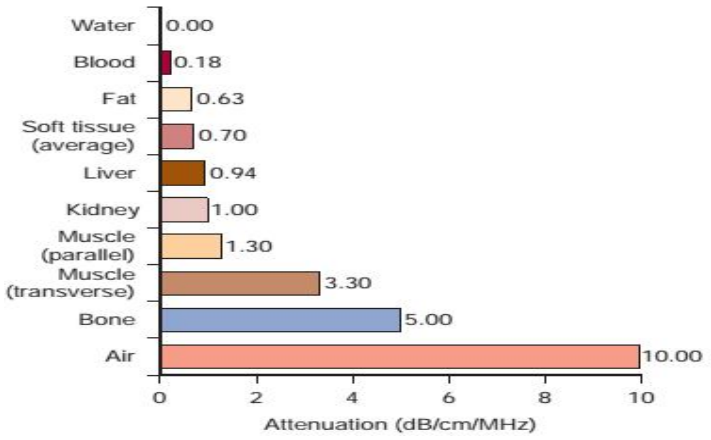

Figure 2.8 Demonstrate attenuation when a sound passes through tissue

2.4.8 Instrumentation:

Ultrasound scanners are complex and sophisticated imaging devices, but all consist of the following basic components to perform key functions:

• Transmitter or pulser to energize the transducer • Ultrasound transducer itself • Receiver and processor to detect and amplify the backscattered energy and manipulate the reflected signals for display • Display that presents the ultrasound image or data in a form suitable for analysis and interpretation • Method to record or store the ultrasound image. **(Peter, 2010)**

2.4.8.1 Transmitter:

Most clinical applications use pulsed ultrasound, in which brief bursts of acoustic energy are transmitted into the body. The source of these pulses, the ultrasound transducer, is energized by application of precisely timed, high-amplitude voltage. The maximum voltage that may be applied to the transducer is limited by federal regulations that restrict the acoustic output of diagnostic scanners. Most scanners provide a control that permits attenuation of the output voltage. Because the use of maximum output results in higher exposure of the patient to ultrasound energy, prudent use dictates use of the output attenuation controls to reduce power levels to the lowest levels consistent with the diagnostic problem.3

The transmitter also controls the rate of pulses emitted by the transducer, or the **pulse repetition frequency** (PRF). The PRF determines the time interval between ultrasound pulses and is important in determining the depth from which unambiguous data can be obtained both in imaging and Doppler modes. The ultrasound pulses must be spaced with enough time between the pulses to permit the sound to travel to the depth of interest and return before the next pulse is sent. For imaging, PRFs from 1 to 10 kHz are used, resulting in an interval of 0.1 to 1 ms between pulses. Thus, a PRF of 5 kHz permits an echo to travel and return from a depth of 15.4 cm before the next pulse is sent.

2.4.8.2 Transducer:

A transducer is any device that converts one form of energy to another. In ultrasound the transducer converts electric energy to mechanical energy, and vice versa. In diagnostic ultrasound systems the transducer serves two functions: converting the electric energy provided by the transmitter to the acoustic pulses directed into the patient and serving as the receiver of reflected echoes, converting weak pressure changes into electric signals for processing.

Ultrasound transducers use **piezoelectricity,** a principle discovered by Pierre and Jacques Curie in 1880. Piezoelectric materials have the unique ability to respond to the action of an electric field by changing shape. They also have the property of generating electric potentials when compressed. Changing the polarity of a voltage applied to the transducer changes the thickness of the transducer, which expands and contracts as the polarity changes. This results in the generation of mechanical pressure waves that can be transmitted into the body. The piezoelectric effect also results in the generation of small potentials across the transducer when the transducer is struck by returning echoes. Positive pressures cause a small polarity to develop across the transducer; negative pressure during the rarefaction portion of the acoustic wave produces the opposite polarity across the transducer. These tiny polarity changes and the associated voltages are the source of all the information processed to generate an ultrasound image or Doppler display. When stimulated by the application of a voltage difference across its thickness, the transducer vibrates. The frequency of vibration is determined by the transducer material. When the transducer is electrically stimulated. a range or **band** of frequencies results. The preferential frequency produced by a transducer is determined by the propagation speed of the transducer material and its thickness. In the **pulsed wave** operating modes used for most clinical ultrasound applications, the ultrasound pulses contain additional frequencies that are both higher and lower than the preferential frequency. The range of frequencies produced by a given transducer is termed its

bandwidth. Generally, the shorter the pulse of ultrasound produced by the transducer, the greater is the bandwidth.

Interference of pressure waves results in an area near the transducer where the pressure amplitude varies greatly. This region is termed the **near field,** or **Fresnel zone.** Farther from the transducer, at a distance determined by the radius of the transducer and the frequency, the sound field begins to diverge, and the pressure amplitude decreases at a steady rate with increasing distance from the transducer. This region is called the **far field,** or **Fraunhofer zone.** In modern multi element transducer arrays, precise timing of the filing of elements allows correction of this divergence of the ultrasound beam and focusing at selected depths. Only reflections of pulses that return to the transducer are capable of stimulating the transducer with small pressure changes, which are converted into the voltage changes that are detected, amplified, and processed to build an image based on the echo information.

2.4.8.3 Receiver:

When returning echoes strike the transducer face, minute voltages are produced across the piezoelectric elements. The receiver detects and amplifies these weak signals. The receiver also provides a means for compensating for the differences in echo strength, which result from attenuation by different tissue thickness by control of **time gain compensation** (TGC) or **depth gain compensation** (DGC). Sound is attenuated as it passes into the body, and additional energy is removed as echoes return through tissue to the transducer. Because echoes returning from deeper tissues are weaker than those returning from more superficial structures, they must be amplified more by the receiver to produce a uniform tissue echo appearance. Another important function of the receiver is the compression of the wide range of amplitudes returning to the transducer into a range that can be displayed to the user. The ratio of the highest to the lowest amplitudes that can be displayed may be expressed in decibels and is referred to as the **dynamic**

range. In a typical clinical application, the range of reflected signals may vary by a factor of as much as 1 : 1012, resulting in a dynamic range of up to 120 dB. Although the amplifiers used in ultrasound machines are capable of handling this range of voltages, gray-scale displays are limited to display a signal intensity range of only 35 to 40 dB.

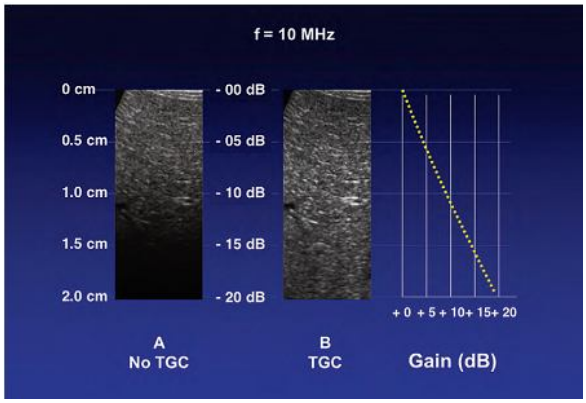

Figure 2.9 Demonstrate the effect of time gain compensation

Compression and remapping of the data are required to adapt the dynamic range of the backscattered signal intensity to the dynamic range of the display Compression is performed in the receiver by selective amplification of weaker signals. Additional manual post processing controls permit the user to map selectively the returning signal to the display. These controls affect the brightness of different echo levels in the image and therefore determine the image contrast. returning signal to the display.

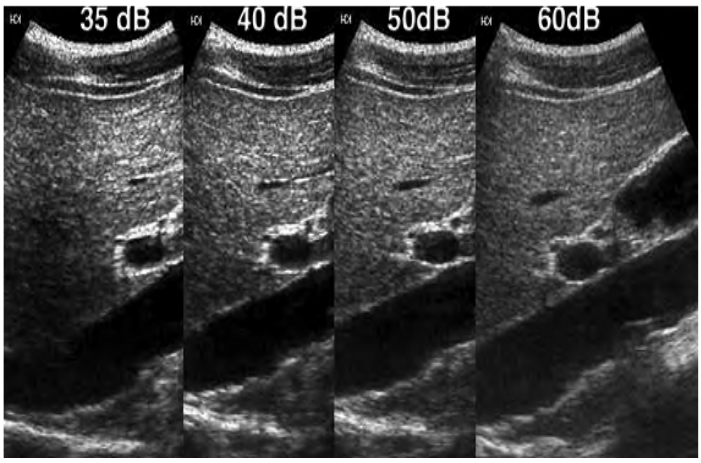

Figure 2.10. Diagram demonstrate the dynamic range

2.4.8.4 Image Display:

Ultrasound signals may be displayed in several ways. imaging has evolved from simple A-mode and bistable display to high-resolution, real-time, grayscale imaging. The earliest A-mode devices displayed the voltage produced across the transducer by the backscattered echo as a vertical deflection on the face of an oscilloscope. The horizontal sweep of the oscilloscope was calibrated to indicate the distance from the transducer to the reflecting surface. In this form of display, the strength or amplitude of the reflected sound is indicated by the height of the vertical deflection displayed on the oscilloscope. With **A-mode ultrasound,** only the position and strength of a reflecting structure are recorded. Another simple form of imaging, **M-mode ultrasound,** displays echo amplitude and shows the position of moving reflectors. M-mode imaging uses the brightness of the display to indicate the intensity of the reflected signal. The time base of the display can be adjusted to allow for varying degrees of temporal resolution, as dictated by clinical application.

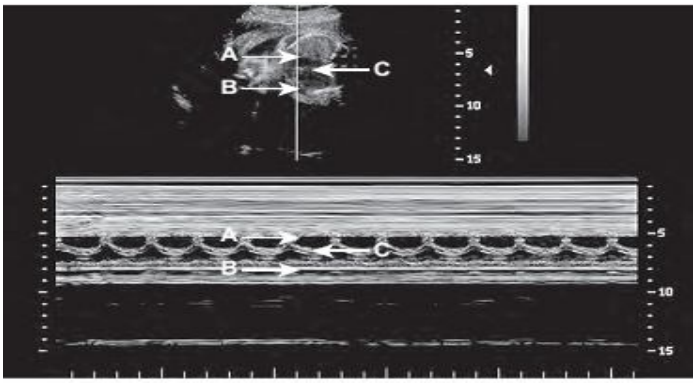

Figure 2.11. Shows M- mode display.

The mainstay of imaging with ultrasound is provided by **real-time, gray-scale, B-mode display,** in which variations in display intensity or brightness are used to indicate reflected signals of differing amplitude. To generate a two-dimensional (2-D) image, multiple ultrasound pulses are sent down a series of successive scan lines, building a 2-D representation of echoes arising from the object being scanned. When an ultrasound image is displayed on a black background, signals of greatest intensity appear as white; absence of signal is shown as black; and signals of intermediate intensity appear as shades of gray. If the ultrasound beam is moved with respect to the object being examined and the position of the reflected signal is stored, the brightest portions of the resulting 2-D image indicate structures reflecting more of the transmitted sound energy back to the transducer. In most modern instruments a digital memory of 512 × 512 or 512 × 640 pixels is used to store values that correspond to the echo intensities originating from corresponding positions in the patient. At least 28, or 256, shades of gray are possible for each pixel, in accord with the amplitude of the echo being represented. The image stored in memory in this manner can then be sent to a video monitor for display. Because B-mode display relates the strength of a backscattered signal to a brightness level on the display device (usually a video display monitor), it is important that the operator understand how the amplitude information in the ultrasound signal is translated into a brightness

scale in the image display. Each ultrasound manufacturer offers several options for the way the dynamic range of the target is compressed for display, as well as the transfer function that assigns a given signal amplitude to a shade of gray. Although these technical details vary among machines, the way the operator uses them may greatly affect the clinical value of the fial image. In general, it is desirable to display as *wide* a dynamic range as possible, to identify subtle differences in tissue echogenicity. Real-time ultrasound produces the impression of motion by generating a series of individual 2-D images at rates of 15 to 60 frames per second. Real-time, 2-D, B-mode ultrasound is now the major method for ultrasound imaging throughout the body and is the most common form of B-mode display. Real-time ultrasound permits assessment of both anatomy and motion. When images are acquired and displayed at rates of several times per second, the effect is dynamic, and because the image reflects the state and motion of the organ at the time it is examined, the information is regarded as being shown in real time. In cardiac applications the terms “2-D echocardiography” and “2-D echo” are used to describe real-time, B-mode imaging; in most other applications the term “real-time ultrasound” is used. Transducers used for real-time imaging may be classified by the method used to steer the beam in rapidly generating each individual image, keeping in mind that as many as 30 to 60 complete images must be generated per second for real-time applications.

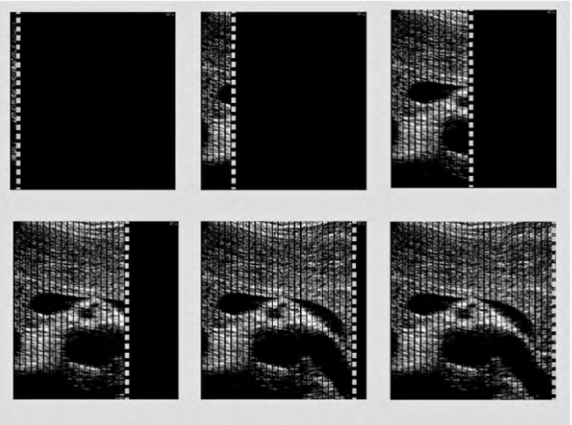

Figure 2.12 Shows B- mode display.

● **Steering** may be done through mechanical rotation or oscillation of the transducer or by electronic means.

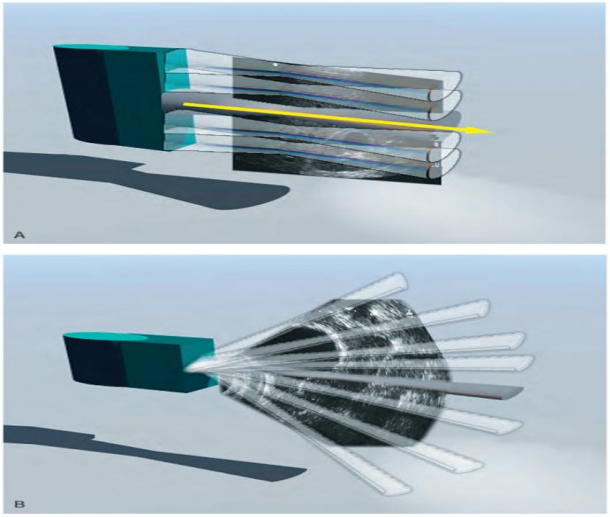

Figure 2.13 Shows beam steering.

Electronic beam steering is used in linear array and phased array transducers and permits a variety of image display formats. Most electronically steered transducers currently in use also provide electronic focusing that is adjustable for depth. **Mechanical beam steering** may use single-element transducers with a field focus or may use annular arrays of elements with electronically controlled focusing. For real-time imaging, transducers using mechanical or electronic

beam steering generate displays in a rectangular or pie-shaped format. For obstetric, small parts, and peripheral vascular examinations, linear array transducers with a rectangular image format are often used. The rectangular image display has the advantage of a larger field of view near the surface but requires a large surface area for transducer contact. Sector scanners with either mechanical or electronic steering require only a small surface area for contact and are better suited for examinations in which access is limited.

2.4.9 Mechanical Sector Scanners:

Early ultrasound scanners used transducers consisting of a single piezoelectric element. To generate real-time images with these transducers, mechanical devices were required to move the transducer in a linear or circular motion. Mechanical sector scanners using one or more single-element transducers do not allow variable focusing. This problem is overcome by using annular array transducers. Although important in the early days of real-time imaging, mechanical sector scanners with field-focus, single-element transducers are not presently in common use.

2.4.9.1 Arrays:

Current technology uses a transducer composed of multiple elements, usually produced by precise slicing of apiece of piezoelectric material into numerous small units, each with its own electrodes. Such transducer arrays may be formed in a variety of configurations. Typically, these are linear, curved, phased, or annular arrays. High-density 2-D arrays have also been developed. By precise timing of the filing of combinations of elements in these arrays, interference of the wave fronts generated by the individual elements can be exploited to change the direction of the ultrasound beam, and this can be used to provide a steerable beam for the generation of real-time images in a linear or sector format. (**Andrew, 2013).**

(A) Linear Arrays: Linear array transducers are used for small parts, vascular, and obstetric applications because the rectangular image format produced by these transducers is well suited for these applications. In these transducers, individual elements are arranged in a linear fashion. By filing the transducer elements in sequence, either individually or in groups, a series of parallel pulses is generated, each forming a line of sight perpendicular to the transducer.

(B) Two-Dimensional Arrays: Transducer arrays can be formed (1) by slicing a rectangular piece of transducer material perpendicular to its long axis to produce a number of small rectangular elements or (2) by creating a series of concentric elements nested within one another in a circular piece of piezoelectric material to produce an annular array. The use of multiple elements permits precise focusing. A particular advantage of 2-D array construction is that the beam can be focused in both the elevation plane and the lateral plane, and a uniform and highly focused beam can be produced. These arrays improve spatial resolution and contrast, reduce clutter, and are well suited for the collection of data from volumes of tissue for use in 3-D processing and display. Unlike linear 2-D arrays, in which delays in the fiing of the individual elements may be used to steer the beam, annular arrays do not permit beam steering and, to be used for real-time imaging, must be steered mechanically.

Transducer Selection Practical considerations in the selection of the optimal transducer for a given application include not only the requirements for spatial resolution, but also the distance of the target object from the transducer because penetration of ultrasound diminishes as frequency increases. In general, the highest ultrasound frequency permitting penetration to the depth of interest should be selected.

For superficial vessels and organs, such as the thyroid, breast, or testicle, lying within 1 to 3 cm of the surface, imaging frequencies of 7.5 to 15 MHz are typically used. These high frequencies are also ideal for intra operative face.

These individual lines of sight combine to form the image field of view Depending on the number of transducer elements and the sequence in which they are field, focusing at selected depths from the surface can be achieved.

(C) Curved Arrays: Linear arrays that have been shaped into convex curves produce an image that combines a relatively large surface field of view with a sector display format. Curved array transducers are used for a variety of applications, the larger versions serving for general abdominal, obstetric, and transabdominal pelvic scanning. Small, high-frequency, curved array scanners are often used in transvaginal and transrectal probes and for pediatric imaging.

(D) Phased Arrays: In contrast to mechanical sector scanners, phased array scanners have no moving parts. A sector field of view is produced by multiple transducer elements field in precise sequence under electronic control. By controlling the time and sequence at which the individual transducer elements are field, the resulting ultrasound wave can be steered in different directions as well as focused at different depths. By rapidly steering the beam to generate a series of lines of sight at varying angles from one side of the transducer to the other, a sector image format is produced. This allows the fabrication of transducers of relatively small size but with large fields of view at depth. These transducers are particularly useful for intercostal scanning, to evaluate the heart, liver, or spleen, and for examinations in other areas where access is limited applications. For evaluation of deeper structures in the abdomen or pelvis more than 12 to 15 cm from the surface, frequencies as low as 2.25 to 3.5 MHz may be required. When maximal resolution is needed, a high frequency transducer with excellent lateral and elevation resolution at the depth of interest is required.

Figure 2.14. Shows Ultrasound transducers for regional blocks. The photograph includes (left to right) broad linear, small footprint linear, curved, sector and hockey-stick transducers. (**Andrew, 2013).**

2.4.10 Image display and storage:

With real-time ultrasound, user feedback is immediate and is provided by video display. The brightness and contrast of the image on this display are determined by the ambient lighting in the examination room, the brightness and contrast settings of the video monitor, the system gain setting, and the TGC adjustment. The factor most affecting image quality in many ultrasound departments is probably improper adjustment of the video display, with a lack of appreciation of the relationship between the video display settings and the appearance of hard copy or images viewed on a workstation. Because of the importance of the real-time video display in providing feedback to the user, it is essential that the display and the lighting conditions under which it is viewed are standardized and matched to the display used for interpretation. Interpretation of images and archival storage of images may be in the form of transparencies printed on film by optical or laser cameras and printers, videotape, or digital **picture archiving and communications system** (PACS). Increasingly, digital storage is being used for archiving of ultrasound images. **(Jane, 2004)**

2.4.10.1 Image quality:

The key determinants of the quality of an ultrasound image are its spatial, contrast, and temporal resolution, as well as freedom from certain artifacts. ***Spatial Resolution***: The ability to differentiate two closely situated objects as distinct structures is determined by the spatial resolution of the ultrasound device. Spatial resolution must be considered in three planes, with different determinants of resolution for each. Simplest is the resolution along the axis of the ultrasound beam, or **axial resolution.** With pulsed wave ultrasound, the transducer introduces a series of brief bursts of sound into the body. Each ultrasound pulse typically consists of two or three cycles of sound. The pulse length is the product of the wavelength and the number of cycles in the pulse. Axial resolution, the maximum resolution along the beam axis, is determined by the pulse length. Because ultrasound frequency and wavelength are inversely related, the pulse length decreases as the imaging frequency increases. Because the pulse length determines the maximum resolution along the axis of the ultrasound beam, **higher transducer frequencies provide higher image resolution**. For example, a transducer operating at 5 MHz produces sound with a wavelength of 0.308 mm. If each pulse consists of three cycles of sound, the pulse length is slightly less than 1 mm, and this becomes the maximum resolution along the beam axis. If the transducer frequency is increased to 15 MHz, the pulse length is less than 0.4 mm, permitting resolution of smaller details. In addition to axial resolution, resolution in the planes perpendicular to the beam axis must also be considered.

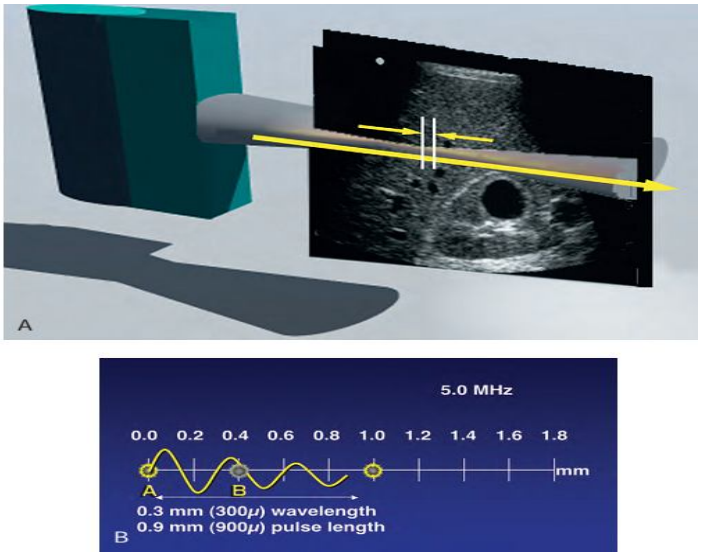

Figure 2.15. Shows Axial resolution.

Lateral resolution refers to resolution in the plane perpendicular to the beam and parallel to the transducer and is determined by the **width** of the ultrasound beam. Azimuth resolution, or **elevation resolution**, refers to the slice **thickness** in the plane perpendicular to the beam and to the transducer. Ultrasound is a tomographic method of imaging that produces thin slices of information from the body, and the width and thickness of the ultrasound beam are important determinants of image quality. Excessive beam width and thickness limit the ability to delineate small features and may obscure shadowing and enhancement from small structures, such as breast microcalcifications and small thyroid cysts. The width and thickness of the ultrasound beam determine lateral resolution and elevation resolution, respectively. Lateral and elevation resolutions are significantly poorer than the axial resolution of the beam. Lateral resolution is controlled by focusing the beam, usually by electronic phasing, to alter the beam width at a selected depth of interest. Elevation resolution is determined by the construction of the transducer and generally cannot be controlled by the user.

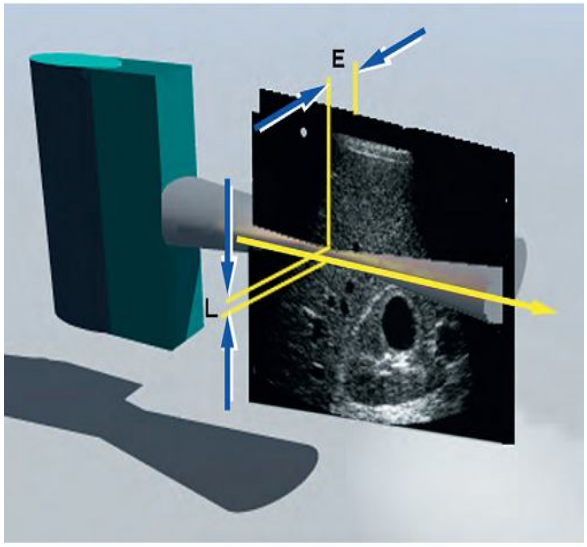

Figure 2.16. Shows lateral resolution.

2.5 Scanning Technique:

The patient is typically examined in the supine position, with the neck extended. A small pad may be placed under the shoulders to provide better exposure of the neck, particularly in patients with a short, stocky habitus. The thyroid gland must be examined thoroughly in both transverse and longitudinal planes. Imaging of the lower poles can be enhanced by asking the patient to swallow, which momentarily raises the thyroid gland in the neck. The entire gland, including the isthmus, must be examined.

The examination must also be extended laterally to include the region of the carotid artery and jugular vein in order to identify enlarged jugular chain lymph nodes, superiorly to visualize submandibular adenopathy, and inferiorly to define any pathologic supra-clavicular lymph nodes. In addition to the images recorded during the examination, some operators include in the permanent record a diagrammatic representation of the neck showing the location(s) of any abnormal findings. This cervical “map” helps to

communicate the anatomic relationships of the pathology more clearly to the referring clinician and the patient. It also serves as a useful reference for the radiologist and sonographer for follow-up examinations.

2.5.1 Thyroid measurement:

With the ellipsoid model, the height, the width, and the depth of each lobe are measured and multiplied. The obtained result is then multiplied by a correction factor,The thickness (anteroposterior measurement) of the isthmus on the transverse view should be recorded.

The volume of each lobe calculate using the equation:

Volume of lobe = Anteroposterior dimension (cm) × Mediolateral dimension (cm) × Craniocaudal dimension (cm) × 0.479.

The thyroid gland volume (TTV) is the summation of the volume of each lobe(Nelson 1987).

2.5.2 Normal Sonographic Appearances:

normal thyroid gland has an homogenous appearance, the capsule may appear as a thin hyperechoic line (Machi , 2005).

2.6 Previous Studies:

This study done by P Vitti et al in 2009 in Tuguegarao and Lagum in Cagayan valley, Philippine established normal thyroid volume in 158 schoolchildren aged 6-12 years using ultrasonography. The mean values of thyroid volume in Tuguerago and Lagum were 2.99 ± 1.34 mL and 2.42 ± 0.92 mL. The thyroid size was significantly in association with age (P < 0.00), weight (P < 0.00), height (P < 0.00), and BSA (P < 0.00) by Pearson's correlation.

Another study done by TT marchie et al 2012 in Benin city, Nigeria establish Normal thyroid volume of 500 school-aged children consisting of 227 boys and 273 girls they found that The US thyroid gland volume ranges between 1.17 cm 3 and 7.19 cm 3 , mean volume range of 1.76-4.95 cm 3 , median volume range of 1.73-4.73 cm 3 , and range of standard deviation from 0.39 cm 3 to 1.49 cm 3. The average mean thyroid volume is 2.32 cm 3 with the following average dimensions; anteroposterior right lobe =1.06 cm, mediolateral right lobe = 1.01 cm and craniocaudal right lobe = 2.34 cm, and anteroposterior left lobe = 1.01 cm, mediolateral left lobe = 1.04 cm and craniocaudal left lobe = 2.41 cm for both boys and girls respectively.

Further more study done by Maryam Moradi et al 2014 in Isfahan, Iran also establish normal thyroid volume of 360 schoolchildren (59% girls) aged 8-15 years they found that Mean thyroid volume measured by US was 1.46 ± 0.70 ml. Thyroid volume in boys was significantly higher than girls (1.58 ± 0.67 ml vs. 1.38 ± 0.71 ml; $P = 0.009$). Thyroid volume was positively correlated with age ($r = 0.25$, $P < 0.001$).

Chapter Three

Materials and Methods

Materials and Methods

3.1 Materials:

This study is Cross –sectional descriptive study aimed to Measurement of Normal Thyroid Gland Volume in School Age Children using Ultrasonography conducted during the period from August to October 2016, at Surgical Diagnostic Center, Kassala state.

There were 64 Childs of age ranged between 6 and 18Years with normal thyroid gland, any child had age younger than 6 and elder than 18years and with clinical evidence of thyroid disease was excluded from this study. Scanning for sample was obtained used high resolution ultrasound machine Mindray M7 color Ultrasound Machine, Sony printer with thermal paper and computer for data analysis.

3.2 Methods:

3.2.1 Ultrasound Technique*: (Imaging protocols)*

The subjects were examined in supine position, with pillow placed under their shoulders to hyperextend the neck. US gel was applied over the thyroid area. The transducer was directly placed on the skin over the thyroid gland, and an image of each lobe was obtained in transverse and longitudinal planes. The craniocaudal and the sagittal dimensions of both lobes were measured on the longitudinal image. The transverse dimension was measured on the transverse image. With the ellipsoid model, the height, the width, and the depth of each lobe are measured and multiplied. The obtained result was then multiplied by a correction factor.

Then measured thethyroid gland volume with the ellipsoid model, the height, the width, and the depth of each lobe are measured and multiplied. The obtained result is then multiplied by a correction factor, The thickness (anteroposterior measurement) of the isthmus on the transverse view should be recorded.

The volume of each lobe calculate individually using the equation:

Volume of lobe = Anteroposterior dimension (cm) × Mediolateral dimension (cm) × Craniocaudal dimension (cm) × 0.479.

The thyroid gland volume (TTV) is the summation of the volume of both lobes.

3.2.2. Methods of data collection:

Using a special data collection sheet (questionnaire), sample of 64 patients with normal thyroid free from any lesion for control groups as well as patient with liver cirrhosis, Hepatitis type B and C were studied by trans abdominal ultrasound scanning and data was collected using a data collecting sheet which designed to evaluate age, gender, thyroid dimensions for each lobe and thyroid volume**.**

3.2.3 Methods of analysis:

Discriminant analysis provides a basis for classifying not only the sample used to compute the discriminant function, but also any other observations that can have value for all the variables by generating a ***classification function***. In this way, discriminant analysis can be used to classify other variables into defined classes. The number of classification functions is equal to the number of classes. Each function allows the computation of a classification score for each variable by applying an equation, which takes the following form:

$$S_i = a_i + \sum_{j=1}^{n} W_{ij} \times V_j$$

where S_i is the resultant classification score for the i^{th} class,

$i = 1, 2, 3...K$ with K being the numbers of classes,

a_i is a constant for the i^{th} class,

$W_{i,j}$ is a weight function for the j^{th} variable for the i^{th} class,

$j = 1, 2, 3...n$ with n being the number of variables.

V_j denotes the value of the j^{th} variable.

Thus, a classification is achieved by multiplying each variable for an individual case by its corresponding weight in the different classes and adding these products together in each class. This process results in a single classification score for each class. Once the classification score is computed, the case is thus classified as belonging to the class in which it has achieved the highest score, and the process is continued in the same fashion for the rest of the variables.

3.2.4 Ethical considerations:

The permission was taken from the head department of ultrasound clinics and data was collected.

All ethical considerations and patient privacy was kept. the patient and his co-patient will be free to decide whether to participate or not. No any patient identification will be published.

Chapter Four

Results

Results

Table (4.1). Shows distribution of participants according to gender

Gender		Frequency	Percent	Valid Percent	Cumulative Percent
Valid	Male	30	46.9	46.9	46.9
	Female	34	53.1	53.1	100.0
	Total	64	100.0	100.0	

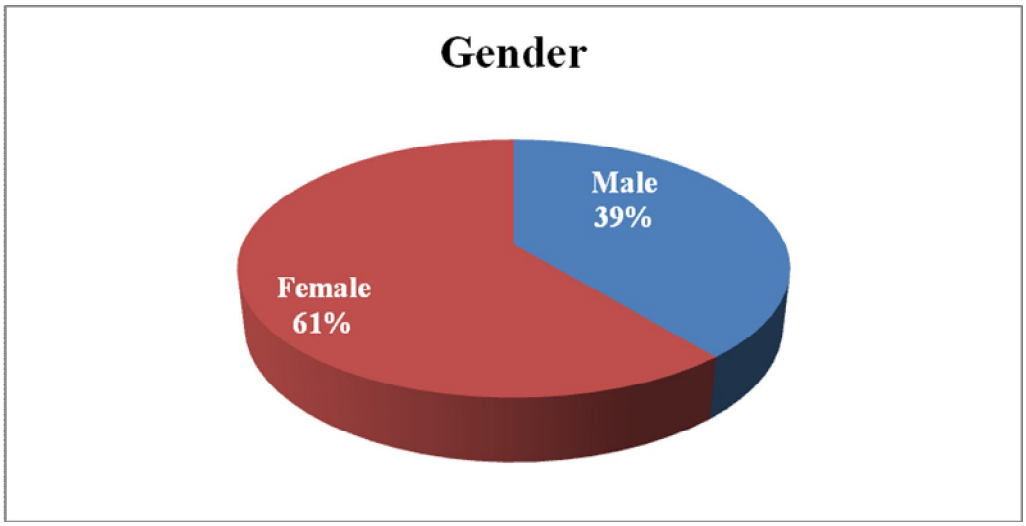

Figure (4.1). Shows distribution of participants according to gender

Table (4.2). Shows distribution of participants according to Age:

Age		Frequency	Percent	Valid Percent	Cumulative Percent
Valid	6	5	7.8	7.8	7.8
	7	6	9.4	9.4	17.2
	8	11	17.2	17.2	34.4
	9	11	17.2	17.2	51.6

	10	7	10.9	10.9	62.5
	11	9	14.1	14.1	76.6
	12	4	6.2	6.2	82.8
	13	7	10.9	10.9	93.8
	14	2	3.1	3.1	96.9
	16	1	1.6	1.6	98.4
	18	1	1.6	1.6	100.0
	Total	64	100.0	100.0	

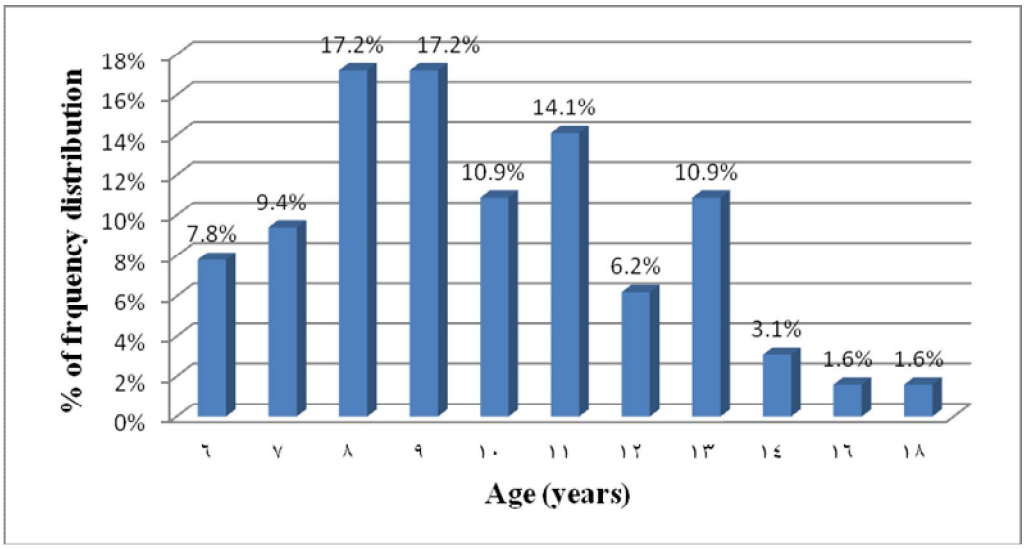

Figure (4.2). Shows distribution of participants according to Age

Table (4.3). Shows Cross tabulation Gender versus Age.

Gender	Age											
	6	**7**	**8**	**9**	**10**	**11**	**12**	**13**	**14**	**16**	**18**	**Total**
Male	2	2	6	5	4	5	0	4	1	0	1	30
Female	3	4	5	6	3	4	4	3	1	1	0	34
Total	**5**	**6**	**11**	**11**	**7**	**9**	**4**	**7**	**2**	**1**	**1**	**64**

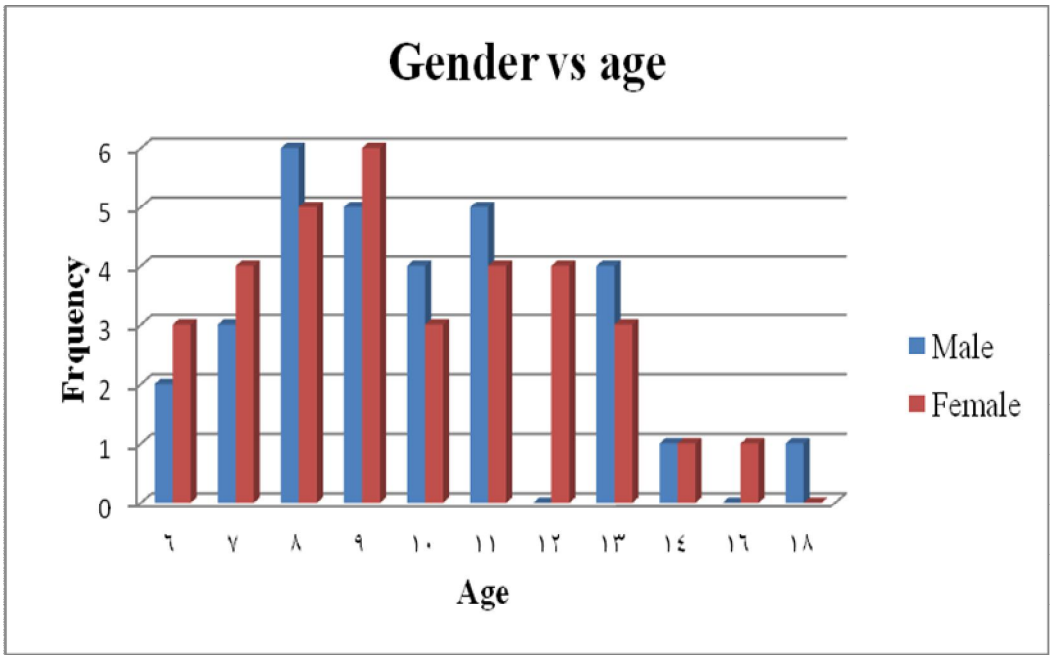

Figure (4.3). Shows Cross tabulation Gender versus Age.

Table (4.4). Shows descriptive of weight variable measurements

	N	Range	Minimum	Maximum	Mean	Std. Deviation
Males	30	90	15	105	33.83	18.888
Females	34	63	12	75	33.35	16.058
Total	64	93	12	105	33.5781	17.302

Table (4.5). Shows descriptive of height variable measurements.

	N	Range	Minimum	Maximum	Mean	Std. Deviation
Males	30	72	110	182	138.07	17.624
Females	34	69	110	179	136.82	16.944
Total	64	72	110	182	137.41	17.139

Table (4.6). Shows descriptive of isthmus measurements.

	N	Range	Minimum	Maximum	Mean	Std. Deviation
Males	30	0.10	0.19	0.29	0.22	0.024
Females	34	0.13	0.19	0.32	0.23	0.033
Total	64	0.13	0.19	0.32	0.22	0.029

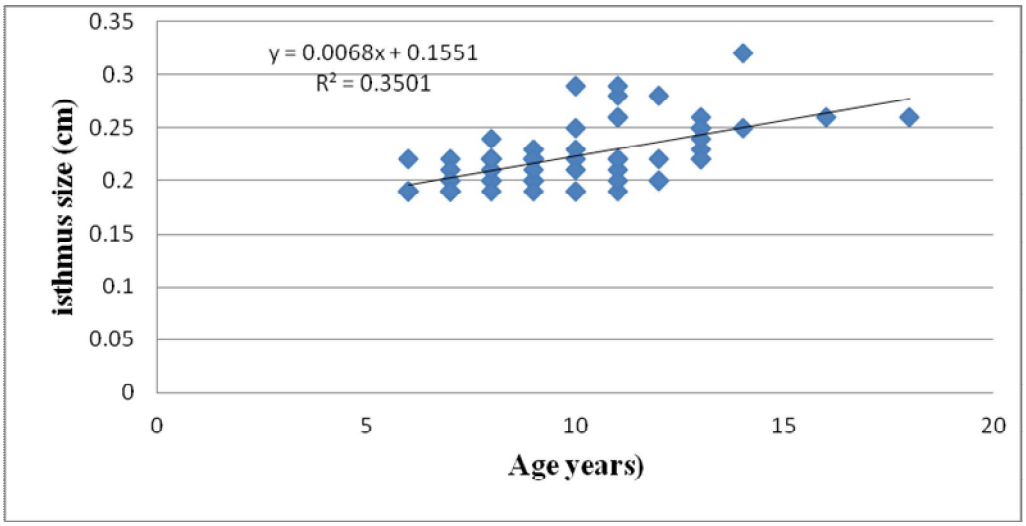

Figure (4. 4) Scatter plot shows a direct linear relation between age and Isthmus sizeof thyroid gland.

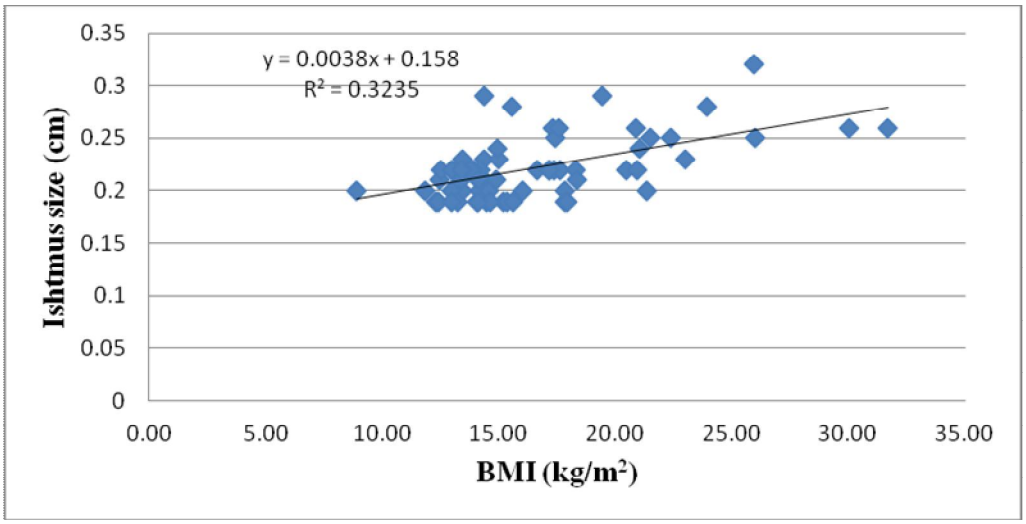

Figure(4. 5) Scatter plot shows a direct linear relation between BMI and Isthmus sizeof thyroid gland.

Table (4.7). Shows descriptive of thyroid gland lobes of the study sample.

	N	R lobe size					L lobe size				
		Range	**Min.**	**Max.**	**Mean**	**Sd.**	**Range**	**Min.**	**Max.**	**Mean**	**Sd.**
Males	30	2.60	1.17	3.77	2.006	0.627	2.97	0.84	3.81	1.847	0.735
Females	34	3.07	1.00	4.07	2.095	0.626	3.00	1.04	4.04	1.965	0.585
Total	64	3.07	1.00	4.07	2.050	0.623	3.20	0.84	4.04	1.910	0.657

Table (4.8). Shows Analysis of variance in right lobes due to gender variable.

Model	**Sum of Squares**	**Df**	**Mean Square**	**F**	**Sig.**
Regression	0.128	1	0.128	0.326	0.570
Residual	24.335	62	0.392		
Total	24.463	63			

Table (4.9). Shows analysis of variance in left lobes due to gender variable.

Model	**Sum of Squares**	**Df**	**Mean Square**	**F**	**Sig.**
Regression	0.221	1	0.221	0.507	0.479
Residual	26.971	62	0.435		
Total	27.192	63			

Table (4.10). Shows analysis of variance in right lobes due age variable

Model	Sum of Squares	Df	Mean Square	F	Sig.
Regression	9.104	1	9.104	36.751	0.000
Residual	15.359	62	0.248		
Total	24.463	63			

Table (4.11). Shows analysis of variance in right lobe due height variable

Model	Sum of Squares	Df	Mean Square	F	Sig.
Regression	11.156	1	11.156	51.978	0.000
Residual	13.307	62	0.215		
Total	24.463	63			

Table (4.12). Shows analysis of variance in right lobe due weight variable.

Model	Sum of Squares	Df	Mean Square	F	Sig.
Regression	10.279	1	10.279	44.930	0.000
Residual	14.184	62	0.229		
Total	24.463	63			

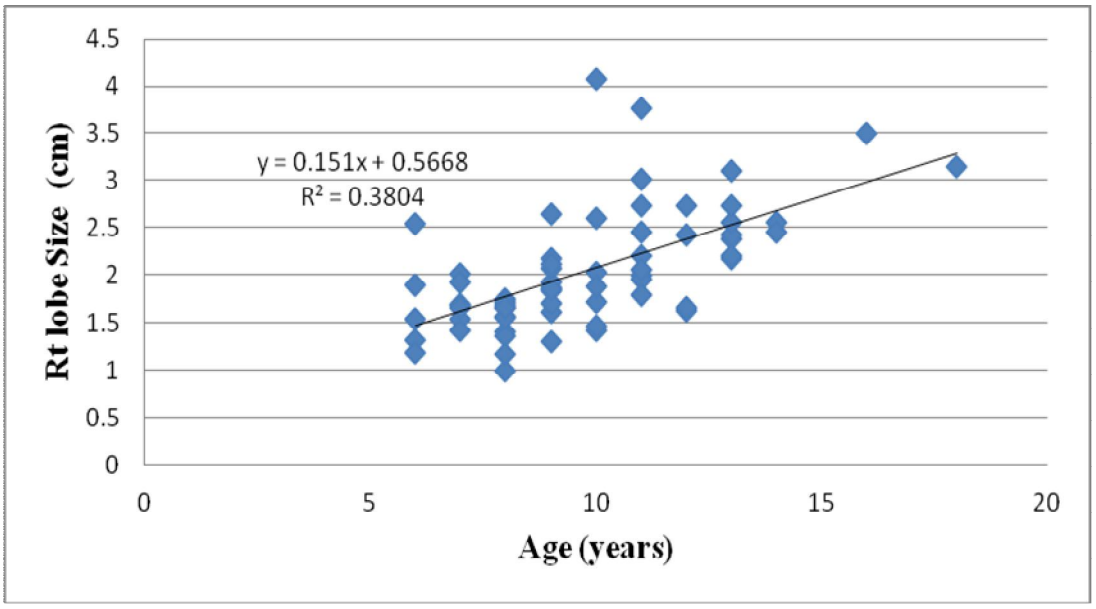

Figuure (4.6) Scatterplot shows a direct linear relation between age and Right lobe sizeof thyroid gland.

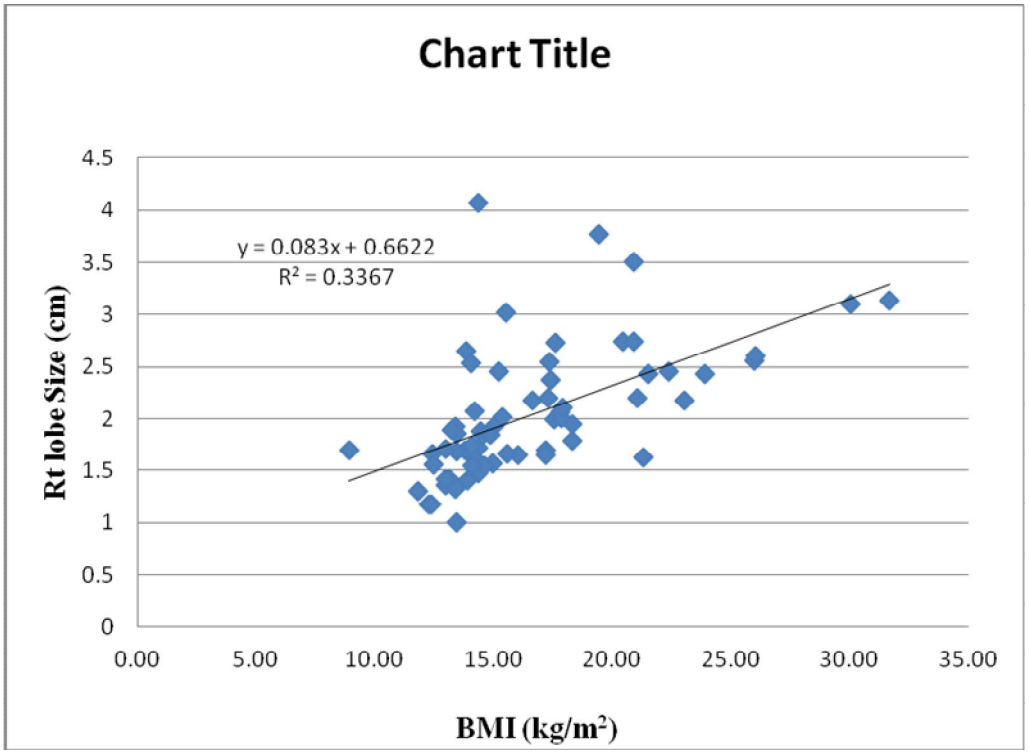

Figure (4. 7) Scatterplot shows a direct linear relation between BMI and Right lobe sizeof thyroid gland.

Table (4.13). Shows analysis of variance in left lobes due age variable.

Model	Sum of Squares	Df	Mean Square	F	Sig.
Regression	9.080	1	9.080	31.080	0.000
Residual	18.112	62	0.292		
Total	27.192	63			

Table (4.14). Shows analysis of variance in left lobe due height variable

Model	Sum of Squares	Df	Mean Square	F	Sig.
Regression	10.969	1	10.969	41.923	0.000
Residual	16.223	62	0.262		
Total	27.192	63			

Table (4.15). Shows analysis of variance in left lobe due weight variable.

Model	Sum of Squares	Df	Mean Square	F	Sig.
Regression	9.373	1	9.373	32.611	0.000[a]
Residual	17.819	62	0.287		
Total	27.192	63			

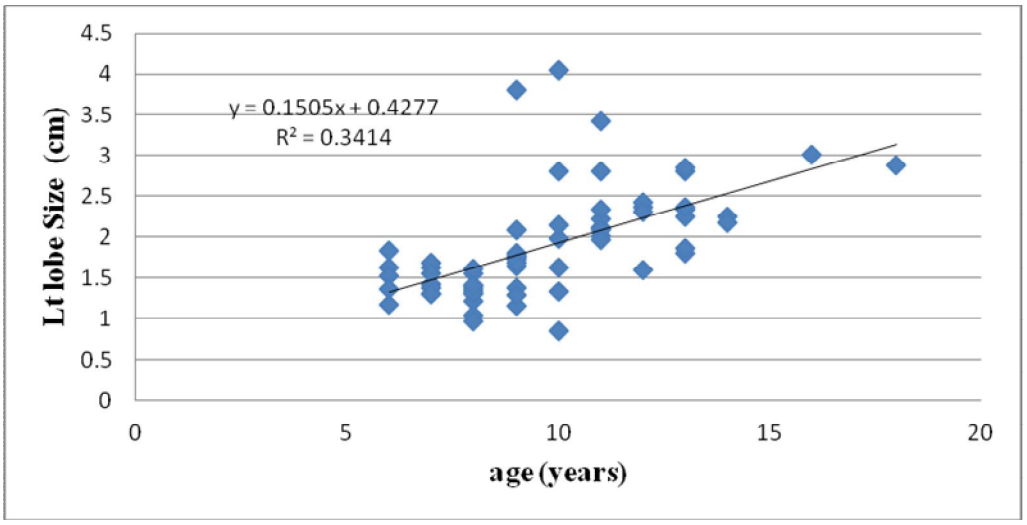

Figuure (4.8) Scatterplot shows a direct linear relation between age and Left lobe sizeof thyroid gland.

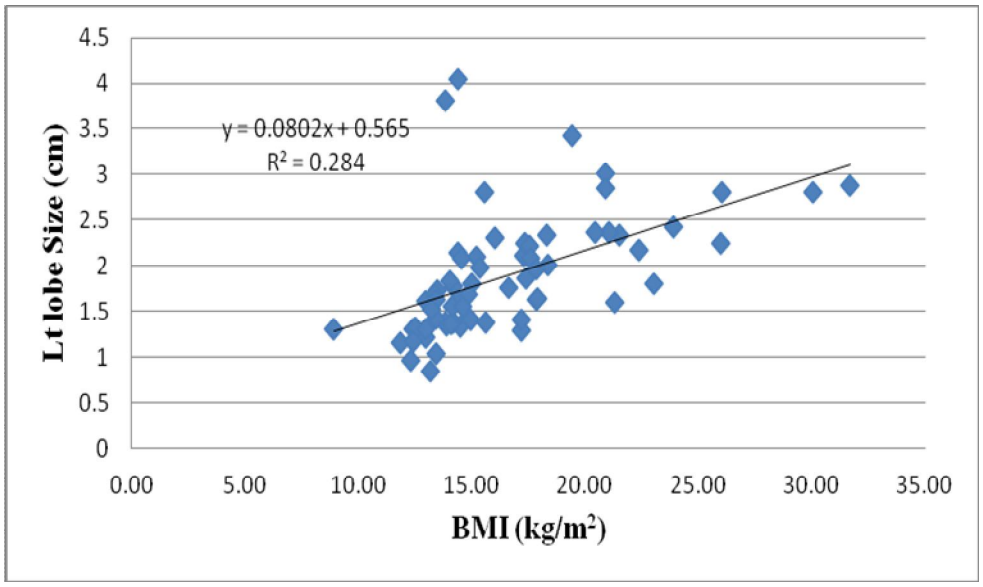

Figuure (4.9) Scatterplot shows a direct linear relation between BMI and Left lobe sizeof thyroid gland.

Chapter Five

Discussion, Conclusion and Recommendations

Discussion, conclusion and Recommendations

5.1 Discussion:

This was a cross sectional descriptive study in which there were 64 subjects had age between (6 to 18 years), 30 cases (46.1٪) out of them were male while other 34 cases (53.1٪) were female as shown in table and figure (4.1), all these Childs were examined using high frequency ultrasound machine.

The mean values for body characteristic height and weight are 138.07±17.6 ,33.83±18.8 and 136± 16.9 ,33.35±16.05 for male and female respectively. The overall mean thyroid gland volume combined for both lobes and sexes obtained from this study was 3.96±1.28 cm^3. There was no previous local study for comparison to the best of our knowledge. Study found that The mean value of right and left lobe size were 2 ± 0.62 , 1.84 ± 0.73 for male and 2.9 ± 0.62 ,1.96 ± 0.58 cm3 for female. In general, the right lobe was larger in size than left one. In Females, measurements show higher average size of two lobes than in the males, same result achieved by (T T Marchie et al, 2012)

Concerning isthmus measurements, there was little variation in measurements in correlation with gender. The mean value for both males and females not differ widely. The mean measurement for male children was (0.22 ± 0.02), while that was (0.23 ± 0.03) for females. Also study found that the size of thyroid Isthmus increased as age of child increased linearly i.e. the Isthmus size increased by 0.01 cm/year of age starting from 0.02 cm. While in case of body mass index the Isthmus increased also linearly by 0.003 $cm/kg/m^2$ starting at 0.2 cm. This results indicates that thyroid Isthmus increased linearly (Direct) as the result of age and BMI increased as shown in figures (4.4,4.5)

Study also revealed that; the size of the right lobe increased as age of child increased linearly by 0.151 cm/year of age starting from 1.0 cm. While in case of body mass index the Isthmus increased also linearly by 0.083 cm/kg/m^2 starting at 1.0 cm. This results indicates that Right lobe of thyroid increased linearly (Direct) as the result of age and BMI increases sigures (4.6 and 4.7). And the size of the left lobe increased as age of child increased linearly i.e. the left lobe size increased by 0.15 cm/year of age starting from 0.7 cm. While in case of body mass index the left lobe increased also linearly by 0.28 cm/kg/m^2 starting at 0.7 cm. This results indicates that Left lobe of thyroid increased linearly (Direct) as the result of age and BMI increases as shown in figure (4.8, 4.9), but there was no statistical significance in right and left lobes volume due to gender variable (table 8.9), all these mean that; there was a statistical significance of difference in right and left lobes measurements due to age and body mass Index, these matched with (Maryam Moradi et al 2014) and (Vitti et al 2009).

5.2 Conclusion:

Study concluded that the overall mean thyroid gland volume combined for both lobes and sexes obtained from this study was 3.96±1.28 cm^3. There was no previous local study for comparison to the best of our knowledge.

Study also found that The mean value of right and left lobe size were 2 ± 0.62 ,1.84±0.73,3 and 2.9±0.62 ,1.96±0.58 cm3 for male and female respectively.

In general, the right lobe was larger in size than left one. In Females, measurements show higher average size of two lobes than in the males.

The study found that no statistical significance in right and left lobes measurements due to gender variable, while there was a statistical significance of difference in isthmus, right and left lobes measurements due to age height and weight (Body Mass Index).

Also study Revealed that the size of thyroid Isthmus increased as age of child increased linearly by 0.01 cm/year of age starting from 0.02 cm. While in case of body mass index the Isthmus increased also linearly by 0.003 $cm/kg/m^2$ starting at 0.2 cm. This results indicates that thyroid Isthmus increased linearly (Direct) as the result of age and BMI increases, ; the size of the right lobe increased as age of child increased linearly by 0.151 cm/year of age starting from 1.0 cm. While in case of body mass index the Isthmus increased also linearly by 0.083 $cm/kg/m^2$ starting at 1.0 cm. This results indicates that Right lobe of thyroid increased linearly (Direct) as the result of age and BMI increases sigures. And the size of the left lobe increased as age of child increased linearly i.e. the left lobe size increased by 0.15 cm/year of age starting from 0.7 cm. While in case of body mass index the left lobe increased also linearly by 0.28 $cm/kg/m^2$ starting at 0.7 cm. This results indicates that Left lobe of thyroid increased linearly (Direct) as the result of age and BMI increased.

5.3 Recommendations:

All people specially child and those who have reduction of Iodine intake were advised to do U/S scanning routinely to exclude the presence of any abnormality, because U/S is a cheep, safety and reliable.

Study recommended that Government should introduce the modern ultrasound machines and increase the training institutes of ultrasound and computer programs for increasing the sonologists skills and experiences

According to the high cost of scientific research which the researcher was faced, the government should appeal universities in Sudan and companies to support the researchers in order to improve plans of treating and management of such diseases.

Further studies should be carried out in this field on many aspects such as increasing the number of patients and introduced other age groups to confirm the relation found in this study between normal thyroid volume with age and body mass index, comparing between the role of U/S scanning and other diagnostic tools using color Doppler ultrasonography.

References

Anele T.2001 Ultrasound volumetric measurement of normal thyroid in Nigerians. *The West African Journal of Ultrasound*.;2(1):10–12.

Archie A, Alexander M. 1996. The thyroid, the parathyroid, the salivary glands and the cervical lymphnodes. In: Goldberg B, Petterson H, editors. *The NICER Year Book* pp. 399–429.

Atlas of Clinical Positron Emission Tomography by Sallie F. Barrington, Michael N. Maisey and Richard R. Wahl. Oxford University Press, Inc. New York, NY. 2006.

Berbel P, Navarro D, Ausó E, Varea E, Rodríguez AE, Ballesta JJ, Salinas M, Flores E, Faura CC, et al. (2010). "Role of late maternal thyroid hormones in cerebral cortex development: an experimental model for human prematurity". Cereb Cortex. 20 (6): 1462–75

Boron WF, Boulpaep E (2003). "Chapter 48: "synthesis of thyroid hormones"". Medical Physiology: A Cellular And Molecular Approaoch. Elsevier/Saunders. p. 1300. ISBN 1-4160-2328-3

Boron, W.F. (2003). *Medical Physiology: A Cellular And Molecular Approaoch*. Elsevier/Saunders. ISBN 1416023283.

Bowen, R. (2000). "Thyroid Hormone Receptors". Colorado State University. Retrieved *22 February* 2015

Brown MC, Spencer R,1978 Thyroid gland volume estimated by use of ultrasound in addition to scintigraphy. *Acta Radiologica: Oncology, Radiation, Therapy Physics and Biology*.17(4):337–341.

Bruneton JN, Balu-Maestro C, Marcy PY, Melia P, Mourou MY.1994 Very high frequency (13 MHz) ultrasonographic examination of the normal neck: detection of normal lymph nodes and thyroid nodules. *Journal of Ultrasound in Medicine*.13(2):87–90.

Brunn J, Block U, Ruf G, Bos I, Kunze WP, Scriba PC, 1981Volumetric analysis of thyroid lobes by real-time ultrasound. *Deutsche Medizinische Wochenschrift.* 106(41):1338–1340.

Brunn J, Block U, Ruf G, Bos I, Kunze WP, Scriba PC. Volumetric analysis of thyroid lobes by real-time ultrasound. *Deutsche Medizinische Wochenschrift.* 1981;106(41):1338–1340.

Büyükgebiz, Atilla (15 November 2012). "Newborn Screening for Congenital Hypothyroidism". Journal of Clinical Research in Pediatric Endocrinology . 4 (4). doi:10.4274/Jcrpe.845

Cummings CW, 1998 ,*Head and Neck Surgery*. 3rd ed. St. Louis, Mo: Mosby; 2445-49.

Dayan CM (February 2001). "Interpretation of thyroid function tests" *Lancet*. 357 (9256): 619–24. doi:10.1016/S0140-6736(00)04060-5.

Fikri m, ashraf f,2011. Clinical ultrasound physics, journal of emergencies, trauma and shock oct-dec;4(4): 501-503.

Iko BO. 1986 Grey scale ultrasonography of the thyroid gland, Nigeria. *Tropical and Geographical Medicine*.;38(1):21–27.

Kwee, Sandi A.; Coel, Marc N.; Fitz-Patrick, David (2007). Eary, Janet F.; Brenner, Winfried, eds. "Iodine-131 Radiotherapy for Benign Thyroid Disease". *Nuclear Medicine Therapy*. CRC Press: 172. ISBN 978-0-8247-2876-2

Machi J, Staren ED. Lippincott Williams & Wilkins. (2005) Ultrasound for Surgeons. ISBN:0781742919.

Massol J, Pazart L, Aho S, Strauch G, Leclere J, Durieux P. 1993, Management of thyroid nodules: preliminary results of a practice survey with 685 general and specialist practitioners. *Annales d'Endocrinologie*. 54(4):220–225.

Nelson M, Wickus GG, Caplan RH, Beguin EA. Thyroid gland size in pregnancy. An ultrasound and clinical study. *Journal of Reproductive Medicine*. 1987;32(12):888–890.

Patrick L (June 2008). "Iodine: deficiency and therapeutic considerations" Altern Med Rev. 13 (2): 116–27. PMID1859034

Ryan SP, Nicholas NMJ.1994 The thyroid and parathyroid glands. In: Ryan SP, Nicholas NMJ, editors. *Anatomy for Diagnostic Imaging*. Philadelphia, Pa, USA: WB Saunders;. pp. 35–37.

Schlögl S, Werner E, Lassmann M, et al. The use of three-dimensional ultrasound for thyroid volumetry. *Thyroid*. 2001;11(6):569–574.

Shabana W, Peeters E, Verbeek P, Osteaux MM,2003 Reducing inter-observer variation in thyroid volume calculation using a new formula and technique. *The European Journal of Ultrasound*. 16(3):207–

Smith, Terry J.; Hegedüs, Laszlo (2016-10-19). "Graves' Disease". New England Journal of Medicine. 375 (16): 1552–1565. doi: 10.1056 /nejmra1510030.

Tahir A, Ahidjo A, Yusuph H.2001 Ultrasonic assessment of thyroid gland size in Maiduguri, Nigeria. *The West African Journal of Ultrasound*. ;3(1):26–31.

Talley, Nicholas (2014). Clinical Examination. Churchill Livingstone. pp. Chapter 28. "The endocrine system". pp 355–362. ISBN 978-0-7295-4198-5

Williams PL, Bannister LH, et al,1995 *Gray's Anatomy*. 38th ed. New York, NY: Churchill Livingstone; 1891-6.

World Health Organization.1994 Indicators for assessing iodine deficiency disorders and their control through salt iodization. World Health Organization, Geneva, Switzerland.

Appendices

Appendix (A)

Data Collection Sheet:

No.	Gender	Age	height	weight	Isthmus size	RTl V	LTL V	No pathology

Appendix (B) U/S images

Appendix (B-1) Thyroid ultrasound image show measurement of thyroid LT lobe dimensions and volume for 10 years female.

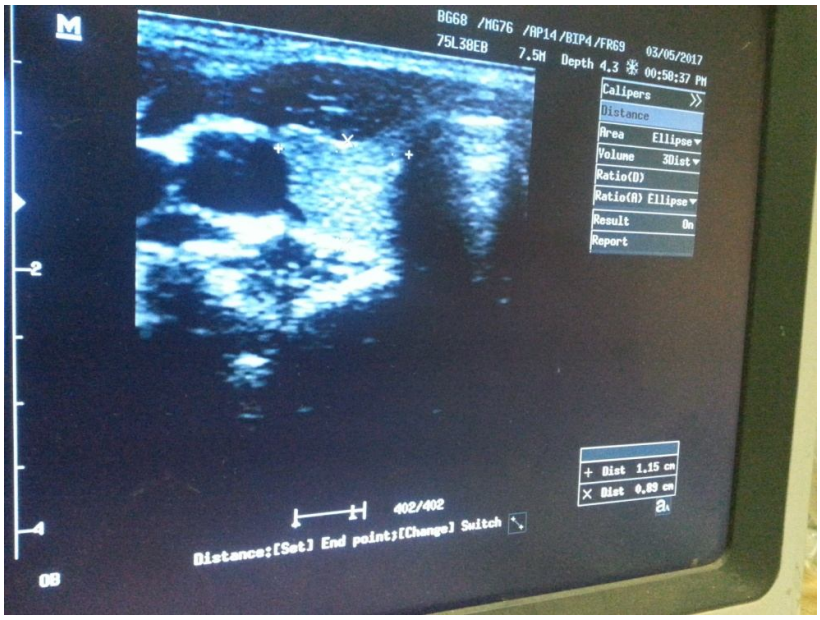

Appendix (B-2) Thyroid ultrasound image show measurement of thyroid RT lobe dimensions and volume for 10 years female.

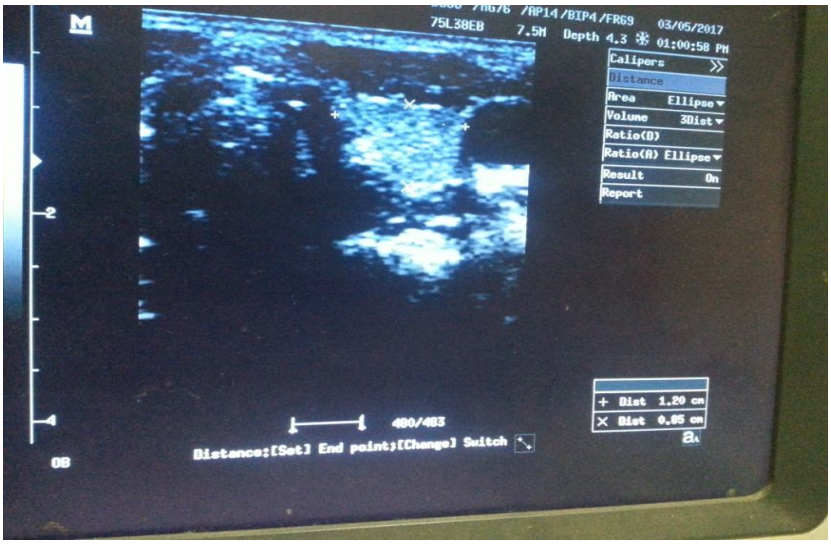

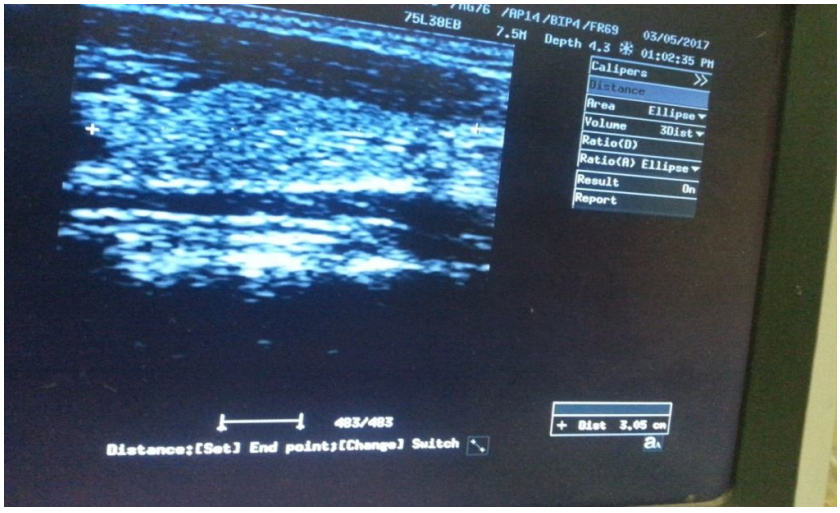

Appendix (B-3) Thyroid ultrasound image show measurement of thyroid LT lobe dimensions and volume for 12 years male.

Appendix (B-4) Thyroid ultrasound image show measurement of thyroid RT lobe dimensions and volume for 12 years male

Appendix (B-5) Thyroid ultrasound image show measurement of thyroid LT lobe dimensions and volume for 8 years male

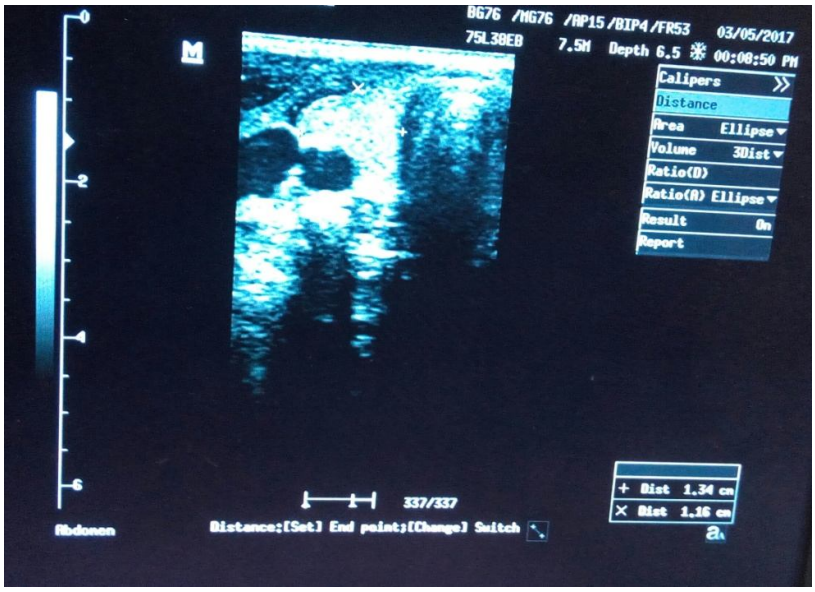

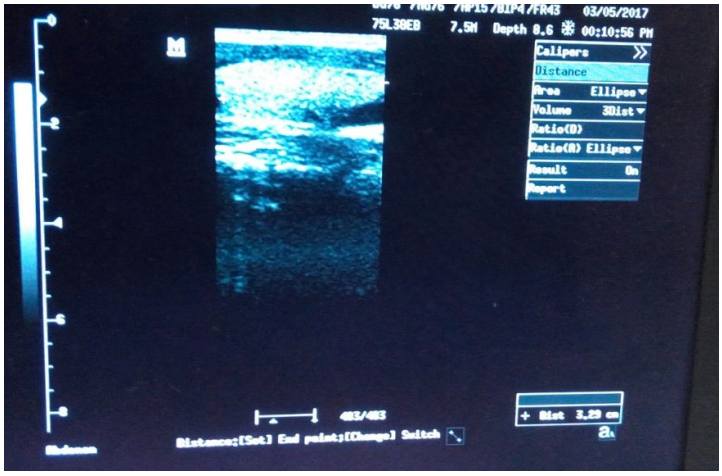

Appendix (B-6) Thyroid ultrasound image show measurement of thyroid RT lobe dimensions and volume for 8 years male.